MATHEMATICS AND MATHEMATICAL MODELLING

Dynamical Models of Plant Growth

N. Bessonov and V. Volpert

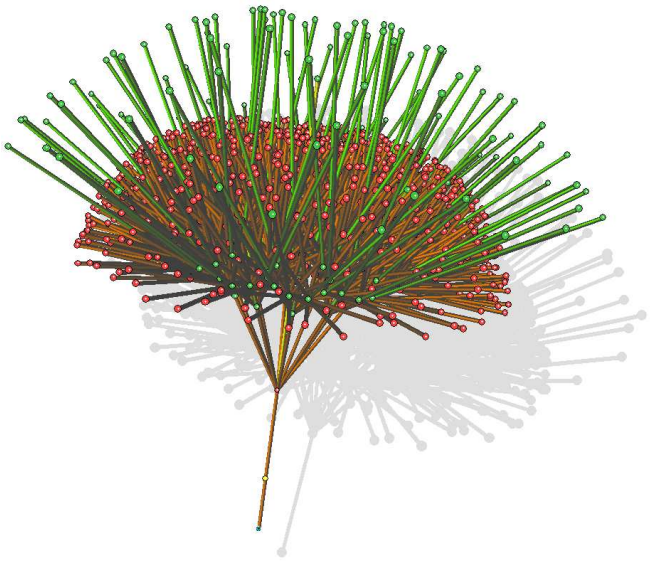

2000 *Mathematics Subject Classification.* Primary 92C80; Secondary 92C15, 35Q80.
Key words and phrases. Plant growth, pattern formation, diversity.

Abstract.

To explain the diversity of plant forms, sizes, and lifetimes, we introduce a new model of plant growth based on simplified but realistic biological mechanisms. Growth of plants is described by means of a free boundary problem where the moving boundary corresponds to the meristem, a narrow layer of proliferating cells. All other plant tissues serve to conduct nutrients and metabolites.

In the one-dimensional model without branching, time oscillations, which can be related to endogenous rhythms, are observed. Periods of growth and rest alternate. The number of growth periods determines the plant size.

Two-dimensional numerical simulations show the emergence of complex structures, and suggest a new mechanism of pattern formation based on the interaction of the moving plant boundary with fluxes inside the plant.

We consider next a one-dimensional model with branching, where the branching condition is determined by concentrations of plant hormones. A wide variety of plant forms is observed. Apical domination, in which growth of one branch suppresses growth of other branches, is studied.

1. Introduction

1.1. Modelling plant growth. Studies of plant growth probably begin from ancient times. In the middle ages, Leonardo da Vinci observed the seasonal periodicity of growth and some features of plant forms ([**21**], pages 239, 912). Theories of phyllotaxis, which can be defined as "a construction determined by organs, parts of organs, or primordia of plants" ([**12**], page 286) appear already in the XVII-th century. D'Arcy Thompson reviewed early theories ([**21**], Chapter XIV) and R.V. Jean contemporary theories of phyllotaxis [**12**].

Phyllotaxis often considers a plant as a given geometrical object without specifying the underlying biological mechanisms that result in the appearance of the observed patterns. There are several approaches in which plants are considered as dynamic objects, which change their size and form over time based on some growth mechanism. The best-known mechanism of pattern formation in mathematical biology is related to reaction-diffusion systems and Turing structures ([**17**], [**16**], and the discussion below). However, there is no biological evidence that this mechanism is really involved in biological pattern formation ([**12**], page 197, [**23**], page 347). Some other approaches use the optimization mechanism. For example, the branching pattern in plants can be related to maximization of light interception [**18**]. Plant topology and design are studied in [**9**], [**5**]. Some other aspects of plant modelling can be found in the Proceedings of the Workshop on Plant Models [**10**]. There are several recent experimental works that establish a relationship between expression of certain genes and formation of plant organs (see e.g. [**20**]).

Another approach to plant modelling is based on attempts to describe the kinetics of plant growth. If $L(t)$ is the plant size that depends on time t, then we can consider the empirical equation

$$\frac{dL}{dt} = F(L), \tag{1.1}$$

where F can be proportional to L (autocatalytic growth), or be some constant (linear growth), or $F(L) = aL(L_0 - L)$, where a and L_0 are parameters (see, e.g., [**11**], [**15**]). Such kinetic equations have been proposed since the early 20th century ([**21**], Chapter III) with no significant progress since then. It is interesting to note that D'Arcy Thompson discusses autocatalytic growth in relation to chemical kinetics and plant hormones.

Such models have several defects. First, they are purely empirical. A formula "which gives a mere coincidence of numbers may be of little use or none, unless it goes some way to depict and explain the modus operandi of growth" ([**21**], page 261). Moreover, they are overly simplified and cannot describe oscillating growth, not to mention branching. And of course, they cannot describe the final plant size, which should be considered as given (L_0 above), or its form. This is what we try to do in this work on the basis of some simplified but realistic mechanisms of plant growth.

1.2. Dynamic models. In this work we model the dynamics of growing plants, i.e., the evolution of their size in time and the emergence of their forms. To suggest

a mathematical model of plant growth, we need to identify the most essential features of the growth mechanism. The simplest and schematic description takes into account nutrients coming from the root along the xylem, metabolites produced by the plant and distributed throughout the plant through the phloem, and plant cells that proliferate and consume nutrients and metabolite.

Model Assumptions

To simplify the modelling, we do not take photosynthesis into account. If we assume that there is enough light and that it is uniformly distributed, then photosynthesis will not be a limiting stage for metabolite production. Therefore it will be implicitly taken into account in the parameters of the model.

Another simplification is that we do not take into account the root growth. We will suppose that the plant begins at the level of the ground. Nutrients are supplied from that level to the plant above.

One of the most important features of plants, for purposes of modelling them, is that proliferating cells are strongly localized. The growing part of the plant where cells divide is called the meristem. The primary or apical meristem is located at the very end of growing shoots and represents a narrow layer of cells with a more or less constant width for each particular plant. The biological mechanism that provides the localization of the apical meristem is related to the expression of certain genes ([**2**], page 1252).

Some parts of the primary meristem can remain in the internodes. Under certain conditions, determined by plant hormones, they can lead to the appearance of buds that can develop into branches. The secondary meristem, or cambium, is responsible for width-wise growth of the plant.

If we consider only the apical meristem, then we can say that cell proliferation and growth determine plant growth. Outside this narrow layer, cells differentiate; they cannot divide any more, and they serve to conduct biological products. Cell division and growth are controlled by external signals called growth and mitosis factors. Each of them is a generic name for a number of biological products. In particular, mitosis factors tell the cell when it should go from a rest state, where it can remain an indefinitely long time, to a division cycle. In some cases, the same molecule can play both roles. In what follows we will not distinguish between these two factors and will call them for brevity GM-factors. They are produced in meristemic cells and can be transmitted between neighboring cells.

The relatively simple structure of plants, where the growing part is strongly localized, suggests very natural mathematical models describing their growth. We describe plant growth with free boundary problems where the motion of the interface corresponds to the displacement of the apical meristem. The speed of the growth, that is of the interface motion, is determined by diffusion and convective fluxes of nutrients in the plant and by a self-accelerating production of plant growth factors in the meristem ([**1**], page 876).

IMPORTANT

Thus the model suggested in this work is based on the following biological facts and mathematical approximations:

1. The growing part of the plant, or apex, contains a narrow exterior part, the meristem where cells proliferate providing the plant growth. This layer has a constant

width and consists of an approximately constant number of cell layers specific to each plant. Since it is very small compared to the whole plant, it will be considered as a mathematical surface. The displacement of this surface corresponds to the plant growth.

2. The appearance of new cells implies that old cells exit this external layer after some time and become a part of the internal plant tissue. They differentiate, that is, they change their functions. They cannot divide any more, and they serve to conduct nutrients to the meristem.

3. The proliferation rate is determined by the concentration of nutrients and of GM-factors in the meristem. The GM-factors are produced in the meristem. The rate of their production is self-accelerating. They can be transmitted between neighboring cells (see [**2**], pages 1254, 1021).

4. Appearance of new buds is determined by concentrations of certain plant hormones ([**11**], page 125; [**19**], page 681). The hormones are produced either in the growing parts of the plant (in our case in the meristem, there are no leaves in the model), or in the root and supplied to the plant above with the flow of nutrients.

Some more specific details of the model will be discussed below.

1.3. Results. 1. 1D case. In the next section we study a one-dimensional model without branching. The growing plant is represented as an interval with its left end point fixed at $x = 0$ and its right end point at $x = L(t)$. The length $L(t)$ is a function of time. Nutrients enter through $x = 0$ and are transported through the interval by convective and diffusive fluxes. The speed of growth $V(t) = L'(t)$ depends on the concentration C of nutrients and on the concentration $R(t)$ of the GM-factor at $x = L(t)$. The production of the GM-factor is described by the equation

$$\frac{dR}{dt} = Cg(R) - \sigma R. \tag{1.2}$$

The typical form of the function $g(R)$ is shown in Figure 1 though we often use a smooth function, σ is a parameter. Its first derivative increases at some interval of R. This allows us to describe an auto-catalytic production of the GM-factor. The second term in the right-hand side of this equation describes consumption or destruction of the factor.

Another essential property of the function $g(R)$ is related to the value of its derivative at $R = 0$. Assuming that the dimensionless concentration C changes between 0 and 1 with $C = 1$ at $x = 1$, we choose $g'(0)$ slightly greater than σ. Therefore, if the concentration C of nutrients at the growing end is small, then the GM-factor will not be produced. Moreover, its concentration will be decreasing. If C is close to its maximal value, then the right-hand side in (1.2) becomes positive, and the concentration of the GM-factor will grow.

The growth rate V is considered as a given function of the GM-factor, $V = f(R)$. For simplicity, we suppose that it is zero for $R \le R_0$ and equals some positive constant for $R \ge R_1 \ge R_0$. Thus, the rate of plant growth equals zero for small concentrations of the GM-factor, and some positive constant for large concentrations.

Boundary Conditions

The growth mechanism can be described as follows. When growth begins, nutrients are consumed at the meristem, that is at $x = L(t)$. Their concentration decreases. When nutrient concentration becomes sufficiently small, the concentration of the GM-factor also decreases since the right-hand side in (1.2) is negative. When GM-factor concentration becomes sufficiently small in its turn, the growth stops since $f(R) = 0$. The nutrients are no longer consumed, and their concentration begins to grow due to diffusion from the root. When it is sufficiently high, the concentration of GM-factor at the meristem starts growing (the right-hand side in (1.2) is positive). When R becomes greater than R_0, a new growth period begins ($f(R) > 0$).

To summarize, we can say that plant growth is determined by the displacement of the apical meristem accompanied by consumption of nutrients and controlled by the GM-factor.

Linear growth vs. Periodic

Numerical simulations show two different modes of growth. We will call them linear and oscillating. The linear mode of growth is characterized by a uniform increase of the length $L(t)$, which is close to a linear function of time. At some moment, the length reaches its final value L_f and does not change any more, the concentration C inside the interval reaches its stationary distribution, the growth speed is zero. The final length of the plant weakly depends on the parameters of the model. From our point of view this mode of growth is not very interesting for biological applications because it does not describe the variety of plant sizes.

In the oscillating mode, periods of growth alternate with periods of rest. During periods of growth, the nutrients are consumed and the concentration of the GM-factor in the meristem is high. During the periods of rest, the concentration of the GM-factor is low, and the concentration of nutrients increases. The number of periods of growth strongly depends on the parameters. It can vary from one to probably infinity. After a number of periods of growth a steady state is reached, and the length $L(t)$ does not change any more.

The increase in length is approximately the same during each period of growth. The final plant length is determined by the number of growth periods. The periods of rest increase with time since a larger plant needs more time to transfer nutrients from the root to the meristem. Oscillations in plant growth can be related to endogenous rhythms, i.e., the rhythms that occur under constant external conditions.

We briefly explain the mechanism of the oscillations. It can be verified that there exist two continuous families of stationary solutions, stable and unstable (see Annexe 3). The solution of the evolution problem approaches first an unstable solution along its stable manifold and then diverges from it along its unstable manifold. Then it approaches in the same way another unstable solution and so on. After several such cycles it finally approaches a stable stationary solution and does not changes after that. The number of cycles depends on the parameters and on the initial conditions.

2. 2D case. The two-dimensional model is based on the same assumptions as the one-dimensional model. However, there are some additional aspects which seem to be rather essential. As we have already discussed, under some simplifying assumptions we can say that plant growth occurs due to cell proliferation and growth in the

apical mersitem. In the two-dimensional case, unlike the 1D case, we should specify the direction of growth. In real plants, when a cell divides, the surface separating two new cells can be approximately parallel to the outer surface of the meristem or perpendicular to it. In the first case the growth occurs into the normal direction to the outer surface, in the second case in the tangential direction. To simplify the modelling we will restrict ourselves to the growth in the normal direction.

The second question concerns the GM-factor production in the meristem. Specifically, when a new cell appears, we need to prescribe to it an initial value of the GM-factor. Different approaches are possible. It seems rather natural, for example, to relate it to its value in the mother cell. It is also known that some information about GM-factors can be transmitted between neighboring cells by means of some signals. It appears that the results of the numerical simulations strongly depend on the choice of the initial value of the GM-factor. This is not surprising because a cell can remain for an indefinitely long time in a rest state waiting for a signal to proceed to the division cycle. Therefore, the time when this signal arrives and its intensity become crucial.

We will discuss this question in more detail in Section 3 and we come to rather surprising conclusions.

The numerical realization of the model becomes much more difficult in the 2D case. Basically, it is related to the necessity to follow the moving free boundary whose form can be very complex, with singularities and with points of self intersection. Moreover, probably one of the key features of the model is that it is not structurally stable in a certain sense and we cannot expect the convergence of the results when decreasing time and space steps. We will discuss this question below.

One of the basic questions of this modelling concerns the mechanism of pattern formation in growing plants. The two-dimensional model developed in this work describes the emergence of complex forms. From the mathematical point of view, this is not related to instability of some stationary solutions and to bifurcations of new solutions. Already in the one-dimensional case we observe time oscillations far from stable stationary regimes to which the solution finally converges.

Appearance of forms in the 2D case corresponds to dynamic instability with a symmetry breaking of transient and not of stationary solutions. The typical situation can be described as follows. Consider the region bounded by two circles with the centers at the origin. The nutrients are supplied through the internal circle while the external one corresponds to the moving boundary. In the beginning, movement remains circular. After some time, when the concentration of nutrients inside the plant decreases and uniform growth cannot be supported any more, the outer boundary splits into growing and unmovable parts giving rise to various forms.

3. 1D case with branching. We model here a growing plant as a system of intervals, which we will call branches. The number and location of branches is not given *a priori*. They will appear and grow according to some rules. In fact, each branch grows according to the same mechanism described above in the one-dimensional case without branching. The difference is that all branches except for

the first one start from another branch and not from the root. The opposite end of the branch corresponds to the apical meristem. The end point of each branch has its own value of GM-factor concentration described by the equation similar to (1.2).

We need to impose two additional conditions on the concentration of nutrients at the points of branching, that is, the point where another branch starts. The first one is the continuity of the concentration, and the second one is the conservation of fluxes (see Section 4). To write this relation, we need to know the relation between cross section areas of branches below and above the branching point. This question also represents an independent interest. It appears that there is conservation of cross section areas asymptotically for a long time. It is satisfied with good accuracy in actual trees.

Appearance of new branches in the model occurs according to the following mechanism. First, there is a new bud that can appear if some conditions on the concentrations of plant hormones are satisfied. The bud is considered as a small branch: it is connected to another branch by one end point, and it has its apical meristem at the other end point. The distribution of nutrient inside the bud and the value of the GM-factor determine whether it starts growing.

We consider two plant hormones in the model. One of them corresponds to auxin and another one to cytokinin. Both are produced in the growing parts of the plant, in our case in the apical meristem, and are transported through the whole plant. It is known that these two hormones play an important role in formation of new buds (see [**11**]). However, the specific form of the branching condition is not known. We discuss this question in Section 4 and suggest branching conditions which seem to give the results in agreement with biological observations.

We observe a wide variety of plant forms and study more specifically the question of apical domination.

2. 1D model without branching

2.1. Model. We consider in this section the one-dimensional case justified if the length (or height) L of the plant is essentially greater than the diameter of its trunk. Hence we consider the interval $0 \le x \le L(t)$ with the length depending on time. The left endpoint $x = 0$ corresponds to the root. Its role is to provide the flux of nutrients taken into account through the boundary condition. We do not model the root growth here. Therefore the left boundary is fixed. The right endpoint, $x = L(t)$ corresponds to the apex. Its width is much less than that of the plant. We suppose in the model that it is a mathematical point. The value $L(t)$ increases over time. According to the assumption above, the growth rate is determined by the concentration of metabolites at $x = L(t)$, which we denote by R. Thus

$$\frac{dL}{dt} = f(R). \tag{2.1}$$

The function $f(R)$ will be specified below.

We recall that the interval $0 < x < L(t)$ corresponds to differentiated cells that conduct nutrients from the root to the apex. We suppose that they are in a liquid solution. Denote by C their concentration, which is a function of x and t. Its evolution is described by the diffusion-advection equation

$$\frac{\partial C}{\partial t} + u\frac{\partial C}{\partial x} = d\frac{\partial^2 C}{\partial x^2}. \tag{2.2}$$

Here u is the velocity of the fluid, and d is the diffusion coefficient. Assuming that the fluid is incompressible and fills the xylem uniformly (the part of the plant tissue conducting nutrients from below to above and located inside the cambium layer), we obtain

$$u = \frac{dL}{dt}.$$

We complete equation (2.2) by setting the boundary conditions

$$x = 0 : C = 1, \quad x = L(t) : d\frac{\partial C}{\partial x} = -g(R)C. \tag{2.3}$$

d = diffusion coeff.

The second boundary condition shows that the flux of nutrients from the main body of the plant to the meristem is proportional to the concentration $C(L, t)$. This is a conventional relation for mass exchange at the boundary, Robin boundary conditions. The factor $g(R)$ shows that this flux can be regulated by proliferating cells. We discuss this assumption as well as the form of the function $g(R)$ below.

We now derive the equation describing the evolution of R. At this point we need to return to the model in which the width of the meristem is finite. We denote it by h. Then we have

$$h\frac{dR}{dt} = g(R)C - \sigma R. \tag{2.4}$$

The first term in the right-hand side of this equation describes production of the GM-factor R in the meristem. The second term corresponds to its consumption.

System of equations (2.1)-(2.4) is a generic one-dimensional model of plant growth based on: a) "continuous medium" assumptions of mass conservation (for $C+R$) and of the proportionality of the flux $\partial C/\partial x$ at the boundary to the value of C; and b) a "biological" assumption that there is a chemical species R, the plant growth and mitosis factor, which is produced in the meristem and which determines the plant growth.

We note that the conservation of mass in the case $\sigma = 0$ implies that the term $g(R)C$ enters both the boundary condition and equation (2.4). Therefore, the assumption that the rate of the plant growth factor production depends on its concentration R makes the boundary condition depend on it also. We will see below that properties of the function g can be crucial for plant growth. In particular, if it is constant (the production rate is not auto-catalytic), we will not be able to describe the essential difference in plant sizes.

We now specify the form of the functions f and g. We will consider f as a piece-wise constant function equal to 0 if R is less than a critical value R_f and equal to some positive constant f_0 if R is greater than R_f (Figure 1a). This means that the growth begins if the concentration of the plant growth factor exceeds some critical value.

The production of the growth factor R is assumed to be auto-catalytic. To simplify the modelling we consider a piece-wise linear function $g(R)$ (Figure 1b). In some cases we also consider smooth functions f and g.

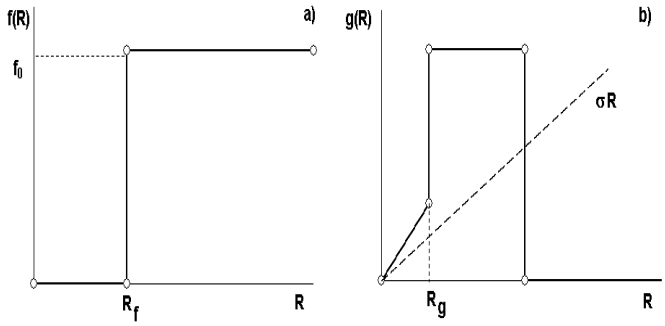

FIGURE 1. Functions f and g.

These assumptions are consistent with plant morphogenesis. It is well known, for example, that auxin, produced in the apex, stimulates mitosis and cell proliferation. Kinetin is also known to stimulate cell proliferation. Production of mitosis factors can be self-accelerating. "The ability of M-Cdk to activate its own activator (Cdc25) and inhibit its own inhibitor (Wee1) suggests that M-Cdk activation in mitosis involves a positive feedback loop ... similar molecular switches operate at various points in the cell cycle to ensure that events such as entry into mitosis occur in an all-or-none fashion" ([**2**], pages 999-1000, see also [**1**], page 876).

2.2. Stationary solutions. In this section we study stationary solutions of the model described in the previous section. Since $f(R) = 0$ in this case, we obtain from (2.2)

$$C(x) = 1 - \frac{1 - C(L)}{L}\, x.$$

Then from (2.3) and (2.4)

$$C(L) = 1 - \frac{\sigma L}{d}\, R.$$

Finally from (2.4)

$$\frac{\sigma R}{1 - \frac{\sigma L}{d}\, R} = g(R). \tag{2.5}$$

This equation should be completed by the condition

$$R < R_f \tag{2.6}$$

such that $L'(t) = 0$.

We assume in what follows that $\sigma < g'(0)$. Then for all L sufficiently large, there exists a solution R of equation (2.5) with condition (2.6). Depending on the function $g(R)$, there can exist more than one solution with the same value of L.

Denote by $F(R)$ the left-hand side in (2.5). The standard linear stability analysis shows that the stationary solution is stable if $F'(R) > g'(R)$ for a solution R.

2.3. Numerical simulations. The functions f and g are characterized by two critical values: the length $L(t)$ increases if $R > R_f$, and the production of R is strongly accelerated if $R > R_g$. The behavior of the system is different in two cases, $R_f > R_g$ and $R_f < R_g$. All simulations are carried out for $d = 0.001$ su^2/tu, $\sigma = 0.009$ su/tu. Here su is a space unit, and tu is a time unit. We will vary h and the initial length L_0.

Relationship between Rg and Rf determines mode of growth

2.3.1. *Linear growth.* If $R_f > R_g$, then the length increase is close to a linear function of time. It reaches its stationary value, and then does not change (Figure 2). The final length L_f weakly depends on h and L_0. For $L_0 = 0.1$ and h from 0.001 to 0.05, L_f changes from 2.54 to 2.50. If $h = 0.001$ and L_0 increases from 0.05 to 0.5, the final length decreases from $L_f = 2.56$ to $L_f = 2.40$.

The value of R_g assumed in the simulations is 0.01. The concentration R is monotonically decreasing over time, approaching its final value ≈ 0.05. Therefore, the results of the simulation remain the same if the function g is identically constant ($g \equiv 0.01$).

2.3.2. *Periodic growth.* The behavior of the solution to problem (2.1)-(2.4) is different if $R_f < R_g$. In this case the growth is periodic in time (Figure 3a). Short periods of growth are separated by long time intervals where the length does not change. The length change is approximately the same during all periods of growth except for the first one, where it is about two times greater. The periods without growth become longer over time. This is related to the growing length of the interval.

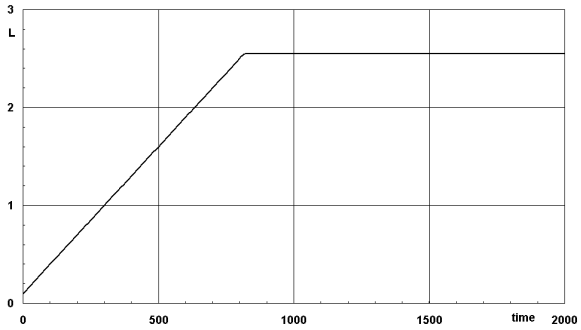

FIGURE 2. Linear growth.

For larger L it takes more time for the concentration $C(L,t)$ to become large enough for $R(t)$ to increase. Figure 3b shows the function $R(t)$.

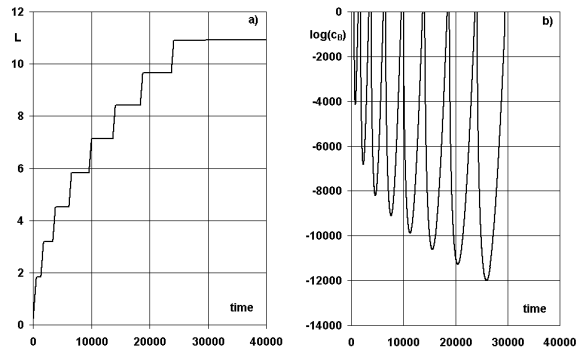

FIGURE 3. Periodic growth.

Contrary to the previous case, the final length L_f is very sensitive to the value of h (Figure 4). For $h = 0.001$ $L_f = 14.56$, for $h = 0.003$, $L_f = 4.19$. The number of periods of growth also varies with h. If for two different values of h the number of periods of growth is the same, then the final length depends on h weakly.

The dependence of the final length on the initial length remains weak. For $h = 0.003$, as L_0 changes from 0.1 to 1.0, L_f changes from 4.19 to 4.61.

We recall that the first boundary condition in (2.3) determines the amount of nutrient available for the plant. The value of the concentration at the left endpoint influences the number of growth intervals and the final plant length. If we decrease the boundary condition, the length also decreases (Figure 4).

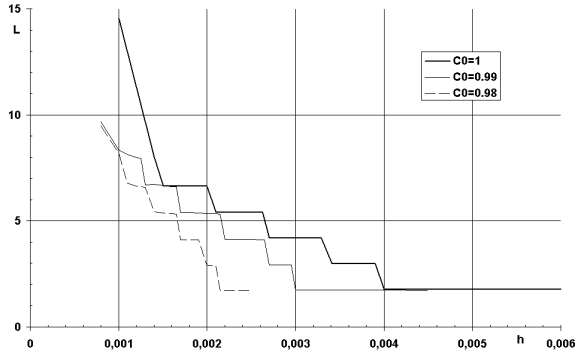

FIGURE 4. Dependence of the final length on h for different C_0.

3. Two-dimensional problem

3.1. Model and algorithm. We formulate the two-dimensional model of plant growth based on the same assumptions as for the one-dimensional model studied in the previous section. To simplify the description of the model, we begin with the geometry shown in Figure 7a. Some other situations will be considered below. The growing plant fills the domain between two closed curves. The internal curve Γ_i is a circle of a fixed radius r with center at the origin. The external curve Γ_e represents the moving boundary. Its local speed will be specified below. The nutrients are supplied through the internal curve, while the meristem corresponds to the external boundary. Its motion describes the plant growth. The region between the two curves is considered as a porous medium. The motion of nutrients is described by the diffusion equation with convective terms

$$\frac{\partial C}{\partial t} + v_x \frac{\partial C}{\partial x} + v_y \frac{\partial C}{\partial y} = d\Delta C, \tag{3.1}$$

where the flow velocity $v = (v_x, v_y)$ is given by the Darcy law

$$v_x = -K\frac{\partial p}{\partial x}, \quad v_y = -K\frac{\partial p}{\partial y}\ . \tag{3.2}$$

Here C is the concentration of nutrients, p is the pressure, d the diffusion coefficient, and $K = k/\mu$, where k is the permeability and μ the viscosity. The liquid is supposed to be incompressible:

$$\text{div } v = 0. \tag{3.3}$$

We next specify the boundary conditions:

$$(x,y) \in \Gamma_i : C = 1, v_x = v_0(t)\cos\alpha,\ v_y = v_0(t)\sin\alpha, \tag{3.4}$$

$$(x,y) \in \Gamma_e : d\frac{\partial c}{\partial n} = -Cg(R),\ v = V_n.$$

Here α is the angle parametrizing the circle Γ_i. The boundary condition for the velocity at Γ_i means that the flow is radial and its velocity equals $v_0(t)$. At the

external boundary, the flow velocity is normal to the boundary and equals the normal velocity V_n of the boundary. The value v_0 depends on time and should be found from the incompressibility and mass conservation conditions:

$$v_0(t) = \frac{1}{2\pi r} \int_{\Gamma_e} V_n(s) ds. \tag{3.5}$$

It remains to specify the motion of the external boundary and the equation for R at the boundary. We suppose that the boundary moves in the direction of the outer normal vector with the velocity being a function of the GM-factor concentration,

$$V_n = f(R), \tag{3.6}$$

where $R = R(x, y, t)$ is determined at the boundary Γ_e. For a given point (x, y) at the external boundary we can consider its trajectory $(x(t), y(t))$ and define the evolution of R by the differential equation

$$\frac{dR(x(t), y(t), t)}{dt} = Cg(R) - \sigma R. \tag{3.7}$$

It generalizes the corresponding equation in the one-dimensional case.

Though the last two relations are rather natural, it is not quite clear how they correspond to biological reality, and they are difficult to realize numerically. Let us first discuss (3.6). One of our basic assumptions is that the motion of the external boundary (the plant growth) occurs due to cell proliferation in the apical meristem. Simplifying the situation, we note that when a cell divides there are two possibilities: one of the two daughter cells can be in the outer layer and another one inside, or they can both be in the outer layer. The first case can be considered as a motion of the boundary in the normal direction, while the second case corresponds rather to the motion in the tangential direction. If we suppose that only the first situation occurs, then the definition of the motion of the external boundary through its normal velocity is justified from the biological point of view. Numerical realization of (3.6) can be related to some difficulties. We do not know *a priori* whether the external boundary is smooth. Singularities can appear even in an initially smooth boundary. Moreover, different parts of the boundary can touch each other. We will see below that the boundary can have a very complex form. Therefore, the motion of the free boundary in the normal direction may not be well defined. An additional difficulty for the discretized problem is to determine the vector normal to the discrete boundary.

Equation (3.7) has a clear biological interpretation: for each cell we can determine all its ascendants from the previous generations and, consequently, define the cell trajectory (cf. [**23**], page 234). Thus, each cell at the meristem moves along its trajectory. If the concentration of the GM-factor R in the daughter cell is determined by its concentration in the mother cell, then equation (3.7) is relevant. However, it is known that in many cases cell communication plays an important role, and the concentration of R in the daughter cell may be determined not only by the mother cell but also by neighboring cells. We will see below that the choice of the initial value of R in new cells essentially influences the results of the simulations.

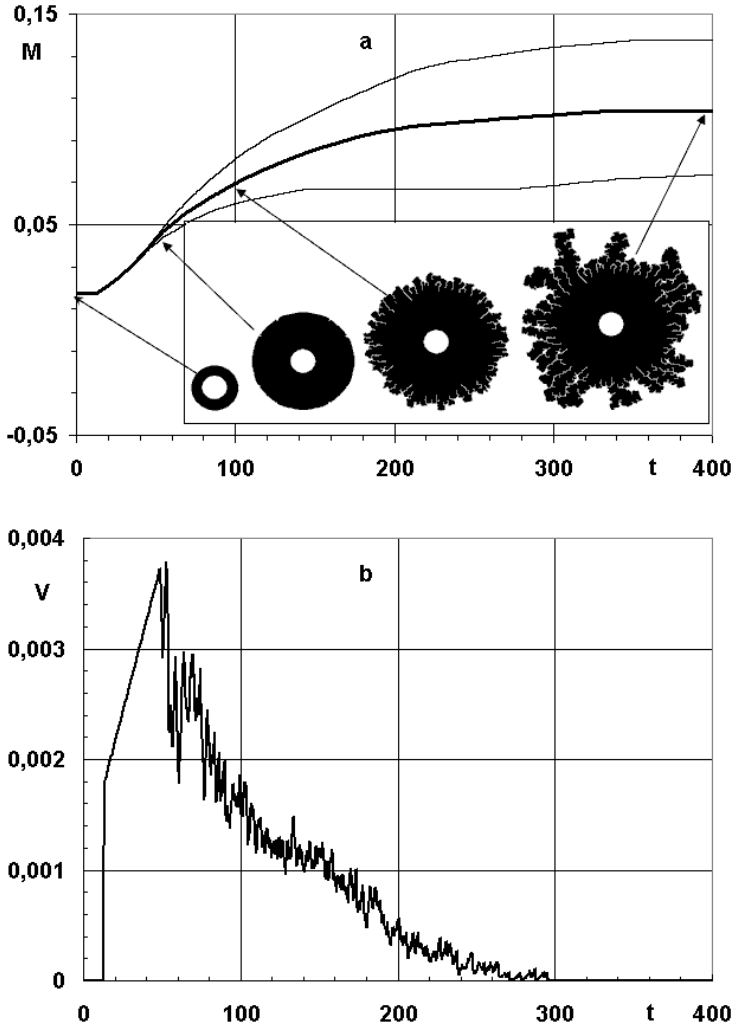

FIGURE 5. a) Total mass as a function of time for three different numerical grids, 101x101 (upper), 201x201 (middle), and 401x401 (lower). Inset: the form of the plant at the corresponding moments of time (t=0,50,100,400) b) Total speed as a function of time for the 201x201 grid.

We note that in the discretized model, which we discuss below, the cells of the numerical mesh do not correspond to biological cells. Therefore, the notion of cell trajectory cannot be directly applied. The functions $x(t)$ and $y(t)$ in equation (3.7)

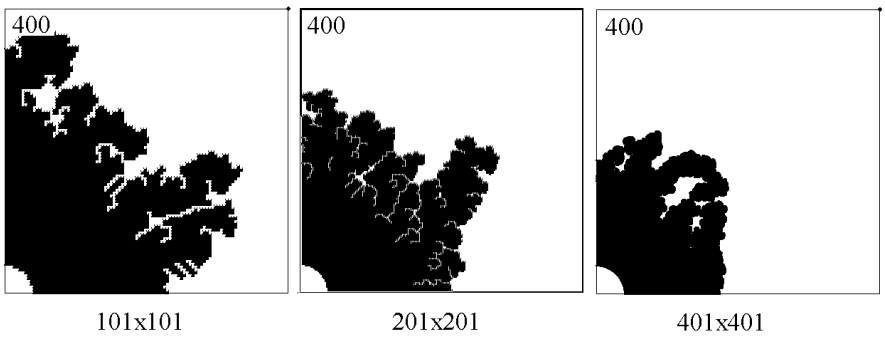

FIGURE 6. Comparison of the results for three numerical grids: 101x101, 201x201, and 401x401 (t=400).

are not defined. Moreover, this equation does not allow us to take into account the exchange of signals between neighboring cells. To overcome these difficulties we will define the motion of the boundary and the equation for R directly in the discretized model. We will see that it will not be a standard discretization of differential equations.

From equations (3.2), (3.3) and the boundary condition (3.4) for the velocity at Γ_e, we obtain

$$\Delta p = 0, \quad \frac{\partial p}{\partial n}|_{\Gamma_e} = \frac{1}{K}\, V_n. \tag{3.8}$$

For numerical simulations we use a finite difference approximation of equations (3.1), (3.8) on the orthogonal grid. We apply the Thomas algorithm to inverse tridiagonal matrices and the alternating direction method to solve the two-dimensional problem.

At each moment of time t_i the domain $\Omega(t_i)$ between the external and the internal boundaries represents a union of square mesh cells. Denote by $\Gamma(t_i)$ the cells from $\Omega(t_i)$ that have at least one common side with a cell outside of $\Omega(t_i)$. Then $\Gamma(t_i) = \Gamma_i(t_i) \cup \Gamma_e(t_i)$, where $\Gamma_i(t_i)$ corresponds to the internal boundary and $\Gamma_e(t_i)$ consists of all other boundary cells.

We define now the motion of the discretized boundary $\Gamma_e(t_i)$. Let C_k be a grid cell from $\Gamma_e(t_i)$ and S_{k1}, S_{k2}, and S_{k3} its sides common with the outer grid cells. We consider a flow from the cell C_k to the neighboring outer cells through the sides S_{kj}. The flow speed is determined by the value $R_k(t_i)$ in C_k. It can be interpreted as a motion of the intervals S_{kj} in the normal direction. When an outer cell is completely filled by the flow, it becomes an inner cell. An outer cell is filled through all its boundaries common with inner cells. The time step is taken to be sufficiently small that a cell can be filled in no less than about 10 steps. Thus, the motion of the discrete boundary is defined in terms of local flows. This approach is applicable for any shape of the boundary.

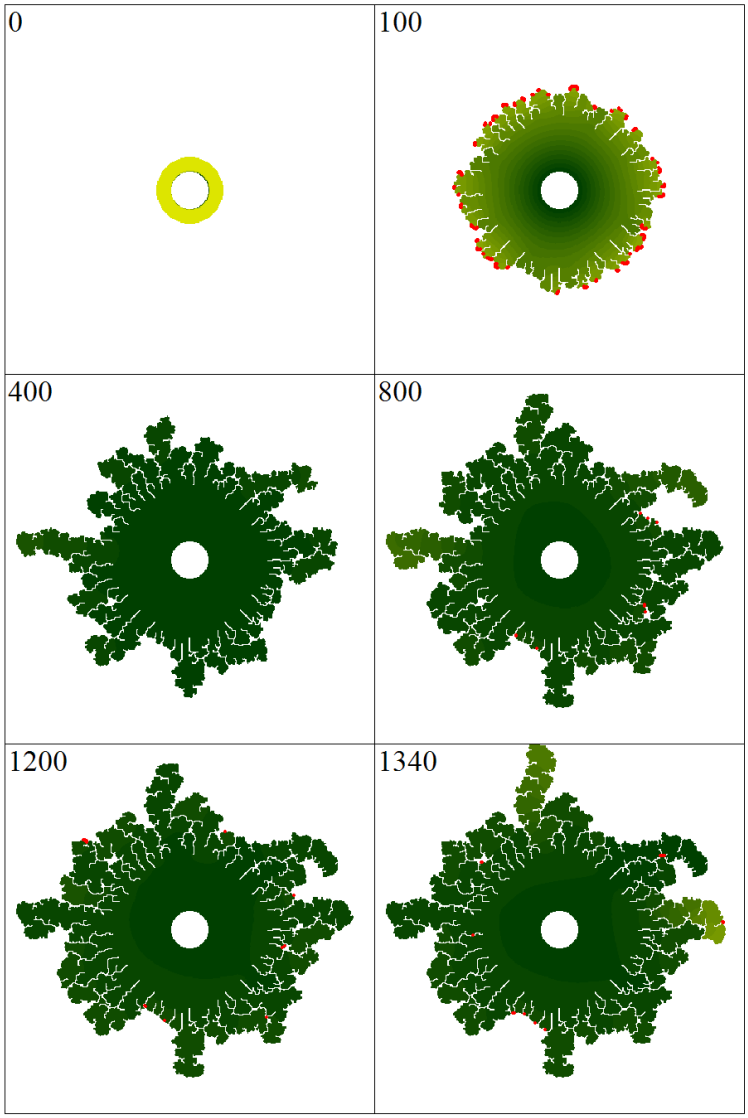

FIGURE 7. The form of the plant in the case without merging in consecutive moments of time. The level of green corresponds to the value of the concentration. Red points show the growing parts ($f_h = 0.003, h = 0.001$.)

The biological interpretation of this law of motion is as follows. Suppose that real biological cells are much smaller than the cells of the numerical mesh. Then the interval S_{kj} is composed of outer surfaces of proliferating cells. This interval moves in the direction of the outer cell with speed determined by the proliferation rate.

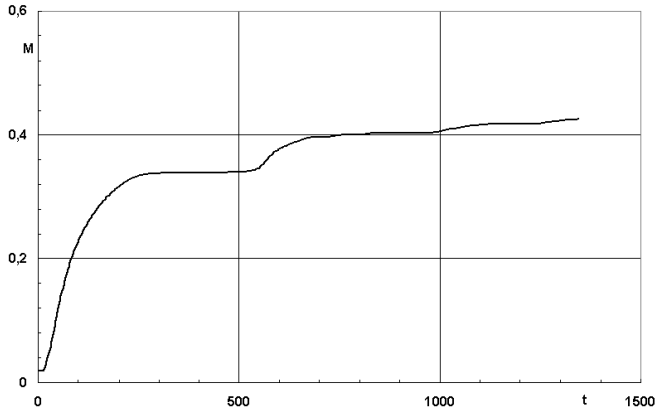

FIGURE 8. Total mass as a function of time for the same simulation.

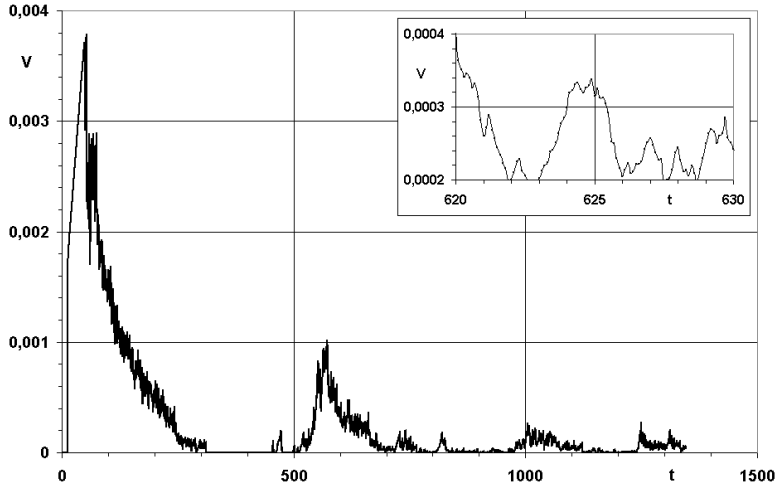

FIGURE 9. Total speed as a function of time for the same simulation.

Therefore, new biological cells fill the outer mesh cell. When this filling occurs from two or three sides of an outer cell, we assume that these processes are independent (e.g., biological cells coming from the left do not feel the cells coming from below). When biological cells completely fill the mesh cell, we consider that it belongs to the domain Ω, that is to the plant. Thus biological cells are small with respect to numerical cells, and the former fill the latter in the process of plant growth.

We define next the evolution of R in the boundary cells. Each boundary mesh cell C_k at each time step t_i is characterized by a value of $R_k(t_i)$. For a given cell C_k,

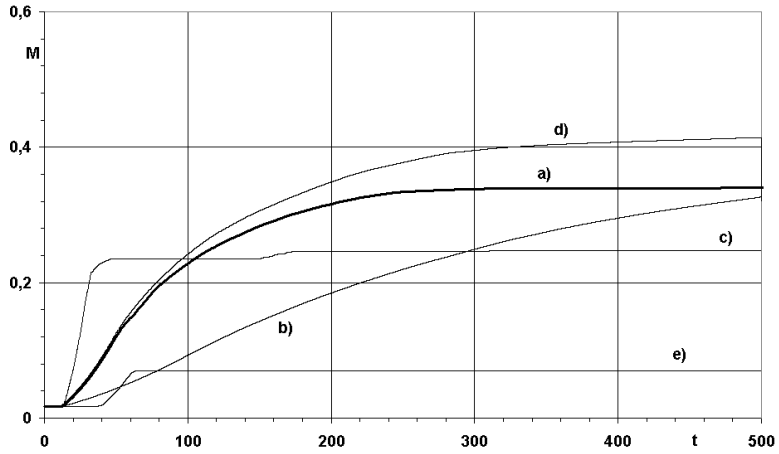

FIGURE 10. Total mass as a function of time for the case without merging: a) $f_h = 0.003, h = 0.001$; b) $f_h = 0.001, h = 0.001$; c) $f_h = 0.01, h = 0.001$; d) $f_h = 0.003, h = 0.0005$; e) $f_h = 0.003, h = 0.005$.

R_k is described by the equation

$$\frac{dR_k}{dt} = Cg(R_k) - \sigma R_k, \tag{3.9}$$

the same as in the one-dimensional case. The uncertainty here is connected with the initial condition for a new cell. Suppose that a cell C_k becomes an inner cell at some time t_i. We should define the value $R_k(t_i)$. In the one-dimensional case the choice is rather obvious: it is the same value as for the "mother" cell at the moment when the "daughter" cell appears. In the two-dimensional case, if the cell C_k is filled from only one inner cell, then we prescribe $R_k(t_i)$ the same value as in the "mother" cell. How $R_k(t_i)$ should be defined when there are two or three "mother" cells? In the case of two "mother" cells, for example,

$$R_{daughter}(t_i) = \Phi(R_{mother,1}(t_i), R_{mother,2}(t_i)),$$

where Φ is some given function. We will see below that the results can strongly depend on the choice of Φ.

3.2. Cell cycle and external signals. Cell growth and division, though determined by complex biochemical processes inside the cell, are controlled by some external signals, usually called growth factors and mitosis factors. In some cases, the same biological products play the role of both factors. Mitosis factors determine the transition of the cell from the resting state G_0, where it can stay an indefinitely long time, to the division cycle. Mitosis and growth factors are produced by meristemic cells and are transmitted to neighboring cells.

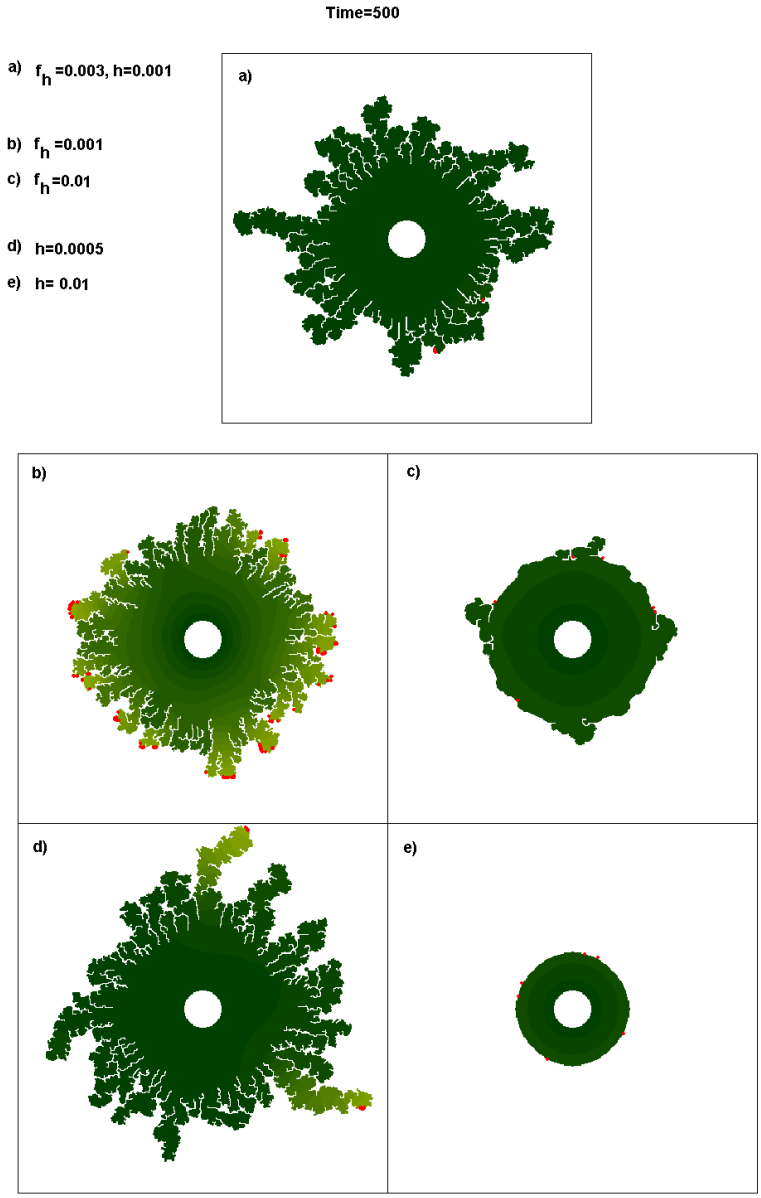

FIGURE 11. The form of the plant at time t=500 in the case without merging.

We do not distinguish two types of factors in the model and consider them as a single variable R. We call it the GM-factor. As it is already mentioned above, our model is based on two assumptions:

1. If the concentration of the GM-factor exceeds a certain value then the plant growth begins. By plant growth we mean both processes, cell growth and division,

2. The GM-factor is produced in a auto-accelerating way (see [**1**], page 876).

One important issue is the initial value of the GM-factor in a new cell. Should it be taken equal to its value in the mother cell, or half of that value, or something different? From our point of view it is determined by external signals. From its inception the cell is submitted to external signals from the neighboring cells. Suppose that a new cell gets signals from two neighboring cells, the left neighbor cell and the right neighbor cell. Let the GM-factor in the left cell have the value R_l and in the right cell R_r. We identify for simplicity the GM-factors and the signals. They come to the cell from the left and from the right and, acting through its membrane receptors, initiate some biochemical reactions inside the cell. These reactions are localized, at least initially, near the cell membrane. Therefore, the actions of the signals R_l and R_r are independent. This means that the equation

$$\frac{dR}{dt} = Cg(R) - \sigma R$$

describing the evolution of the GM-factor inside the cell should be considered with two different initial conditions, $R(0) = R_l$ and $R(0) = R_r$. Only the larger value will be essential since it will first reach the critical value and will initiate mitosis. Hence we set $R(0) = \max(R_l, R_r)$.

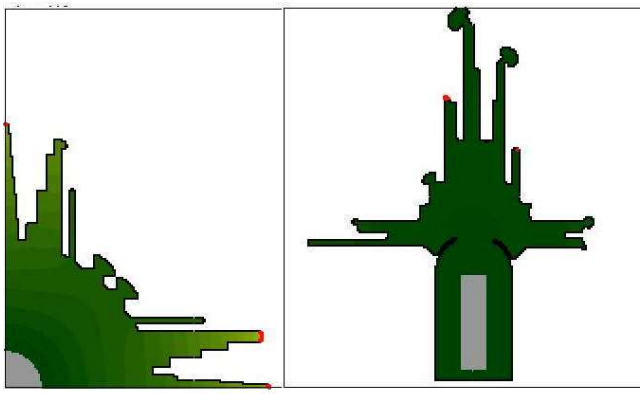

FIGURE 12. Simulations with the initial value of R equal the arithmetic mean of the values of R for mother cells.

We note that we do not identify numerical cells with biological cells. However, we have the same issue for the numerical cells as for biological cells: when a new cell appears we need to prescribe to it an initial value of R. Following the discussion above, we will take the maximum among neighboring numerical cells unless something

else is explicitly indicated. Most of the numerical simulations are carried out with this initial condition.

It appears that the results of the simulations strongly depend on the initial value of R. If instead of $\max(R_l, R_r)$ we take for example $(R_l + R_r)/2$, then the results are quite different (cf. Figures 6, 12, 17). The time evolution is more or less the same at the first stage where the growth is uniform. At the second stage, where boundary cells behave in some sense as coupled oscillators, the initial value becomes crucial. In the case of the arithmetic mean, the preferential directions of the numerical mesh are clearly visible in the results (Figure 12). That is not the case for the maximum (Figure 6, 17).

We can conclude that the case of maximum is more justified biologically and behaves better numerically. We do not know whether it is an occasional coincidence. We will see below that some other cases can be also of interest.

3.3. Time evolution. In this section we discuss the case without merging. This means that when two parts of the moving boundary touch each other, they stop and do not become internal points of the domain. The fluxes and the flow cannot cross it.

In the case of radially symmetric initial conditions there are two clearly different stages of growth. Figure 7 shows the shape of the growing domain in several consecutive moments of time. In the beginning the outer boundary of the domain remains circular. It grows with the same speed in all directions. After some time the growth becomes nonuniform and some spatial structures emerge. The red points show the parts of the external boundary where growth occurs at this moment.

In what follows we will use two characteristics of growth: total speed $V(t)$ and total mass $M(t)$. By total speed we mean the integral of the local speed over the whole external boundary, by the total mass the area of the domain. Both of them depend on time. Figure 5 shows the the total mass (a) and the total speed (b) as functions of time. At the first stage of growth, the total speed is a linear function of time. In fact, the local velocity is constant and the length of the external boundary increases linearly. Their product gives the total speed.

At the second stage of growth the total speed is strongly oscillating. Clearly, these oscillations are not numerical because the time step $\Delta t = 0.1$ is much less than the characteristic time of the oscillations (see Figure 9). On the other hand, it is not related to the evolution of the individual mesh cell because there are several dozen of them growing simultaneously. Thus, it could be synchronized oscillations of individual mesh cells. The analogy with coupled oscillators is only limited because the mesh cells, like biological cells, can stop growing and remain in a rest state for a long time waiting until the concentration R becomes sufficiently high.

Existence of high frequency oscillations in growing plants is well known and has already been discussed by D. Thompson ([**21**], pages 171, 237). Moreover, there are very different time scales for the oscillations. The characteristic time can be on the order of seconds, minutes, days, or months. We cannot give here a clear explanation

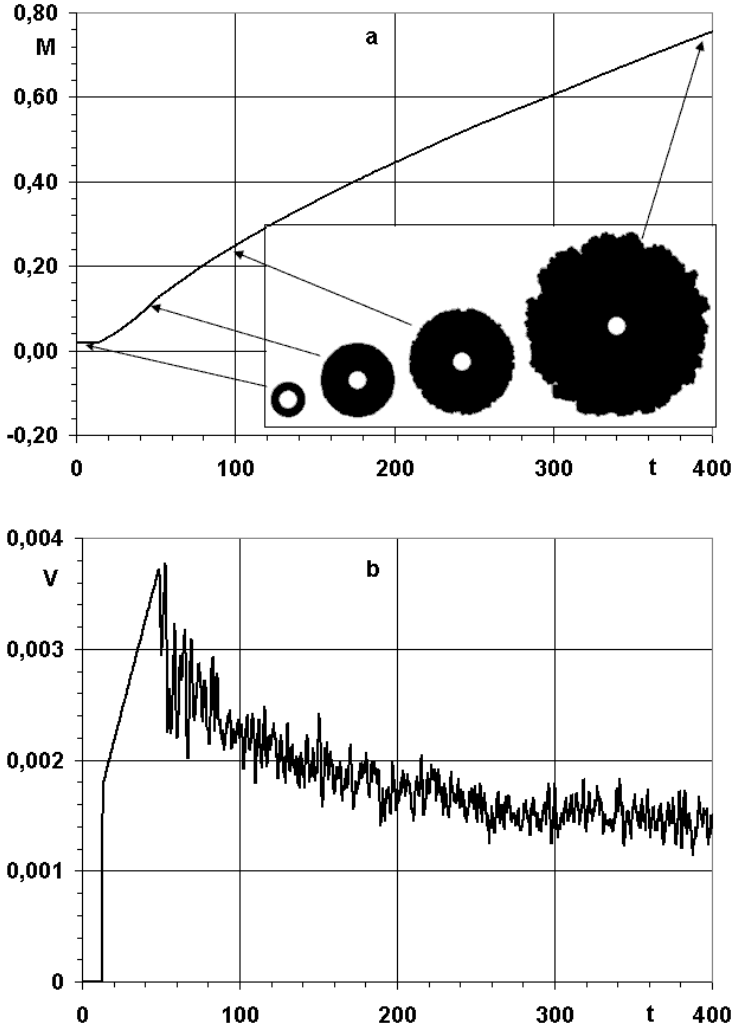

FIGURE 13. a) Total mass as a function of time in the case of merging. Inset: the form of the plant at the corresponding moments of time (t=0,50,100,400); b) Total speed as a function of time.

of this phenomenon, but we observe oscillations with different time scales in the numerical simulations (see Figure 9).

Figures 7-9 show the time evolution of the structure, of the total mass and of the total speed for $f_h = 0.003$. The level of green corresponds to the concentration of nutrients coming from the internal circle where $c = 1$. At the growing parts of the

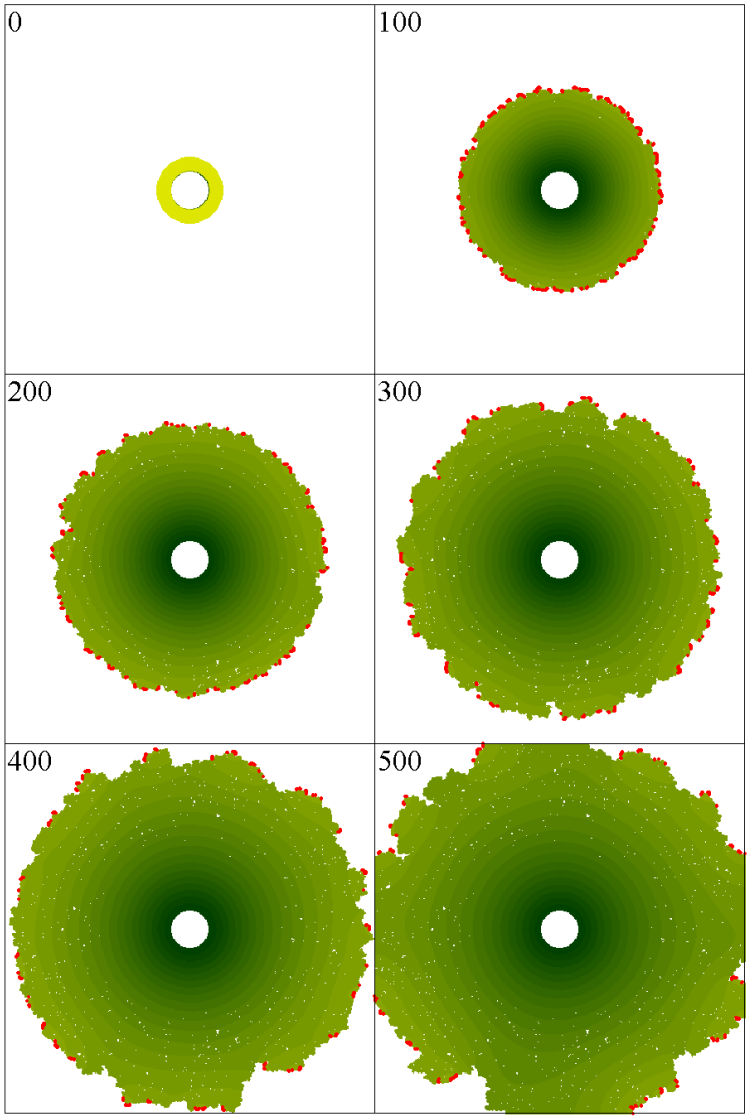

FIGURE 14. Evolution of the plant form in the case with merging. The level of green corresponds to the value of the concentration. Red points show the growing parts.

boundary shown with red points, the concentration is about 0.4. When the supply of the nutrients is not sufficient and their concentration drops, the right-hand side of the equation for R becomes negative. The value of R decreases, and the growth stops. After that, nutrients are not consumed any more at this part of the boundary and their concentration starts increasing.

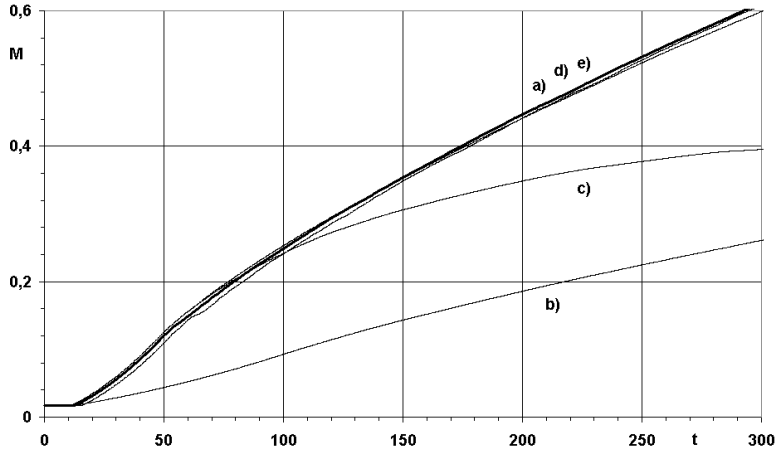

FIGURE 15. Total mass as a function of time for the case with merging: a) $f_h = 0.003, h = 0.001$; b) $f_h = 0.001, h = 0.001$; c) $f_h = 0.01, h = 0.001$; d) $f_h = 0.003, h = 0.0005$; e) $f_h = 0.003, h = 0.005$.

For the simulations shown in Figure 7, the growth stops at $t = 300$, then after some time it begins again. After $t = 700$ growth is continuous albeit sometimes very slow.

3.4. Time and space steps, other parameters. The usual test of numerical accuracy consists of decreasing the time and space steps. Figure 5a shows the total mass as a function of time for different space steps. At the first stage of growth, in which growth is uniform, the evolution of the total mass over time for the numerical grids 100×100, 200×200, and 400×400 is the same.

At the second stage of growth, in which growth is not uniform, the qualitative behavior of the function $M(t)$ for different space steps is the same. However, there is no convergence of the results as the step decreases. This is not related to the numerical accuracy in the usual sense.

Figure 6 compares the form of the plant for a given time with different space steps. Though the results do not coincide, the characteristic size of spatial structures remains the same.

The absence of convergence as the time and space steps decrease means that they should be considered as parameters of the problem.

Figure 10 show the results of the simulations for different values of the parameters f_h and h. The value of f_h determines the local growth speed. Figures 11a, b, and c show the corresponding structures at the same moment of time $t = 500$. The characteristic angular size of the structures is less when f_h is decreased.

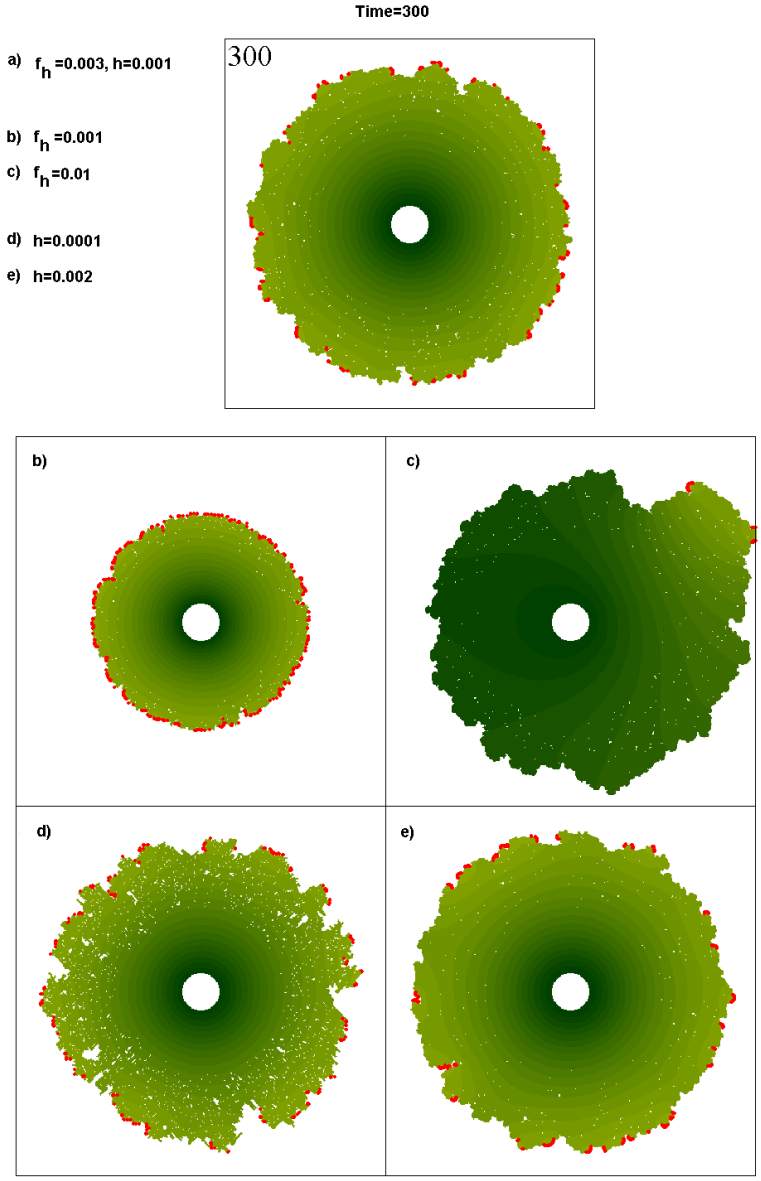

FIGURE 16. The form of the plant at time t=300 in the case with merging.

At the first stage of growth, the total mass increases faster for large f_h. However, growth practically finishes rather abruptly, though there can still exist several red points. For large t the total mass becomes larger when the local growth speed is less.

We recall that h corresponds to the width of the meristem. Decreasing it two times does not essentially change either the structure or the evolution of the total mass in time. However, for $h = 0.01$ (Figure 11e) the behavior is different. The growth stops before spatial structures appear.

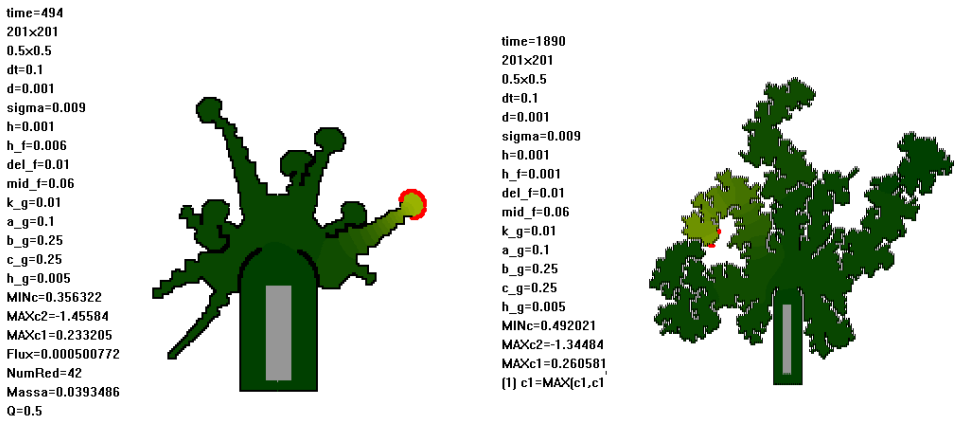

FIGURE 17. Simulations with different initial values of R.

3.5. Other geometries. Figure 17 shows two other examples. The example on the right is computed with the same model as before but in a different geometry. The nutrients are supplied through the internal rectangle. Growth is prevented from the lateral and lower sides of the external rectangle. Only the upper part can grow.

The figure at the left is obtained for another function Φ. The initial value of R for a new cell is taken as some linear combination between the maximum and the arithmetic mean value. The growth pattern becomes rather different. There are several shoots appearing one after another. Some time later a circular extension appears at the end of each shoot. Its evolution in time is shown in Figures 31 and 32 (for the left image in Figure 17).

3.6. Growth with merging. In the process of plant growth, two parts of the moving boundary can touch each other. In this case two boundary mesh cells have a common side. The common side can be considered either as a boundary of the domain or its internal points. The former case was considered above. For the latter, the concentration flux and the fluid flow can pass through it. We call this process growth with merging, and discuss it in this section.

Figures 13 shows the evolution over time of the total mass (a) and of the total speed (b). We observe the same type of high frequency irregular oscillations as before.

The evolution of the plant form is shown in more detain in Figure 14. As before, the level of green corresponds to the value of the concentration, and the red points at the external boundary show growing parts.

Emerging structures here are less pronounced than in the case without merging, for the obvious reason that internal boundaries disappear when two parts of the boundary meet each other. It should be noted that small holes remain inside the plant. The growth stops there and probably will not start again.

In Figure 16 the structure of the plant is compared for the same value of time and for different values of parameters f_h and h. It is interesting to note that the structure becomes more porous for small h (Figure 16d).

Figures 15 shows the evolution of the total mass over time for different values of the parameters. The value of h influences it weakly. The total mass is more sensitive to the value of f_h. It appears that the total mass is maximal for the intermediate value of this parameter ($f_h = 0.003$). It becomes less both for greater and for lesser values.

4. 1D model with branching

4.1. Branching conditions. In this section we discuss conditions of appearance of branches in the framework of the one-dimensional model of plant growth. We use the experimental observation on shoot and root growth from calus: if the concentrations of two hormones, auxin and cytokinin (which we denote by A and K, respectively) are in a certain proportion, then shoots will appear. For a different proportion, not shoots but roots will grow [**11**], [**19**].

Hormone A is produced in growing parts of the plant (leaves, shoots); hormone K in either roots or in growing parts. In our model, A will be produced at the moving boundary $x = L$ that corresponds to the apical meristem. The rate of production is proportional to the growth rate.

Hormone K will either be supplied solely through the stationary end of the interval $x = 0$ (the root) or will also be produced at the moving boundary.

Let us discuss several questions that will allow us to formulate the branching conditions.

1. For any fixed moment of time the distributions of the hormones $A(x,t)$ and $K(x,t)$ considered as functions of x determine a continuous curve on the plane (A,K). If the condition for appearance of new branches is given by a relation between A and K,

$$F(A,K) = 0,$$

for example $A/K = \alpha$, where α is a given value, then the branching condition determines the second curve on the (A,K)-plane. In the generic case, if these curves intersect, they are not tangent at the intersection point. Since the first curve is continuous with respect to time, and the second curve does not depend on time, then they will intersect during some time interval. Therefore we will have not one but many branches appearing at some space interval. Moreover, if we decrease the numerical time step and check the branching conditions at every time step, then the number of appearing branches will increase.

Thus the condition for branching should not be given by a relation between A and K, that is by a curve on the (A,K)-plane, but by conditions on A and K,

$$A = A_0,\ K = K_0, \tag{4.1}$$

where A_0 and K_0 are some given concentrations. In this case it will be a point on the (A,K)-plane. The curve $(A(x,t),K(x,t))$ moving with time on the (A,K)-plane can pass through this point. Each such passage will produce a branch.

This is a structurally stable, generic situation in which we can have a discrete set of branches.

2. The second question is from where the hormone K is supplied, $x = 0$ or $x = L$.

Consider first the case where it is $x = 0$. There are two possible situations. If we keep the concentration of K at $x = 0$ constant, and if it is not consumed in the plant, that is for $x > 0$, then it will rapidly fill the whole interval. The concentration will be

practically constant everywhere for $x > 0$, and, consequently, the critical conditions become independent of K.

The second case is where the K is consumed inside the interval. The equation for K becomes

$$\frac{\partial K}{\partial t} = d\frac{\partial^2 K}{\partial x^2} - V\frac{\partial K}{\partial x} - \mu K.$$

For a constant V (growth rate) there is a stationary solution of this equation, which is exponentially decreasing in x. Even if V changes, the distribution of K will be more or less localized near $x = 0$. For sufficiently long plants it will not influence the critical conditions of branching near the growing part.

Thus we come to the second conclusion: the hormone K, which participates in the critical conditions of branching, should be produced in the growing part of the plant.

3. Consider now the case where both hormones A and K are produced at the moving interface. Suppose first that it moves with a constant speed. Then after some time the distributions of A and K will be exponential in x and moving with a constant speed together with the interface. Let $t = t_0$. If for some $x = x_0$ the branching condition (4.1) is satisfied, then it will be also satisfied for all $t > t_0$ and for $x = x_0 + V(t - t_0)$. Therefore, we will have an infinite number of branches appearing behind the growing part of the plant.

How we can obtain a discrete set of branches? It is known that auxin and cytokinin can be produced by a bud. Therefore, their concentrations will be changed in the vicinity of the newly formed bud, the branching conditions will no longer be satisfied, and there will not be another bud nearby.

4.2. Model. The concentrations of nutrients C, and of hormones A and K are described by the diffusion equations with convective terms:

$$\frac{\partial C}{\partial t} + V\frac{\partial C}{\partial x} = d_C\frac{\partial^2 C}{\partial x^2}, \tag{4.2}$$

$$\frac{\partial K}{\partial t} - V_K\frac{\partial K}{\partial x} = d_K\frac{\partial^2 K}{\partial x^2} - \mu K, \tag{4.3}$$

$$\frac{\partial A}{\partial t} - V_A\frac{\partial A}{\partial x} = d_A\frac{\partial^2 A}{\partial x^2} - \mu A. \tag{4.4}$$

The convective speed V in the first equation is determined as the speed of growth:

$$\frac{dL}{dt} = V, \quad L\Big|_{t=0} = L_0, \quad h\frac{dR}{dt} = Cg(R) - \sigma R, \quad R\Big|_{t=0} = R_0, \quad V = f(R) \tag{4.5}$$

Here d_C, d_K, d_A and μ are parameters; the space variable x is defined independently for each branch. The convective speed V_A in equations (4.3) and (4.4) can be different in comparison with equation (4.2). It corresponds to transport in the phloem in the direction from top (meristem) to bottom (root).

The boundary conditions for C are the same as in the case without branching:

$$C\Big|_{x=0} = C_0, \quad d_C \frac{\partial C}{\partial x} + Cg(R)\Big|_{x=L} = 0. \tag{4.6}$$

The boundary conditions for K describe its possible production in the root, and its production in the meristem with rate proportional to the rate of growth:

$$K\Big|_{x=0} = K_0, \quad d_K \frac{\partial K}{\partial x}\Big|_{x=L} = \varepsilon V. \tag{4.7}$$

Finally, the boundary conditions for A are similar, except that the boundary condition at $x = 0$ takes into account that this horomone can be transported from the stem to the root:

$$\frac{\partial A}{\partial x} - \beta A\Big|_{x=0} = 0, \quad d_A \frac{\partial A}{\partial x}\Big|_{x=L} = \varepsilon V. \tag{4.8}$$

We define next the branching conditions. A new branch appears at $x = x_0$ and $t = t_0$ if

$$A(x_0, t_0) = A_b, \quad K(x_0, t_0) = K_b, \tag{4.9}$$

where A_b and K_b are some given values. Appearance of a new branch means that there is an additional interval connected to the previous one at its point x_0. The variables C_n, A_n, K_n and R_n are described at the new interval by the same equations as above. Here the subscript n determines the number of the branch. We should complete the formulation by the initial value of the concentration $R_n = R_n(t_0)$. It cannot be found as a solution of the problem but should be considered as a parameter.

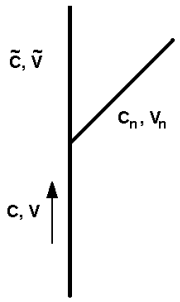

FIGURE 18. Schematic representation of convective and diffusion fluxes in 1D plant with branching.

There are additional branching conditions for the concentrations

$$C_n(0, t) = C(x_0, t), \quad A_n(0, t) = A(x_0, t), \quad K_n(0, t) = K(x_0, t),$$

which means that the concentrations are continuous at branching points. We also need some conditions on the fluxes to provide the conservation of mass. Under the notations shown in Figure 18, we have

$$SV = \tilde{S}\tilde{V} + S_n V_n, \quad S\frac{\partial C}{\partial x} = \tilde{S}\frac{\partial \tilde{C}}{\partial x} + S_n \frac{\partial C_n}{\partial x}.$$

Here $S, \tilde{S}$, and S_n are parameters determined by the cross section area of the corresponding branch (see Annexe 2). For example, if all branches have the same cross section, then $S = \tilde{S} = S_n = 1$. If the cross section areas are conserved and narrow branches have the same diameter, then $S = 1$, and $\tilde{S} = S_n = 1/2$.

In this work we restrict ourselves to the case where all branches have the same cross section. Otherwise, the diameter of each branch should be considered as a function of time. The diameter would depend on fluxes of metabolites coming through the branch to the root. On the other hand, the fluxes of nutrients going through the branch from the root would depend on its cross section. We obtain a very complex time-dependent problem with many feedbacks. This will essentially complicate the understanding of the mechanism of growth and the interpretation of the results.

As is discussed in the previous section, bud formation is accompanied by production of A and K.

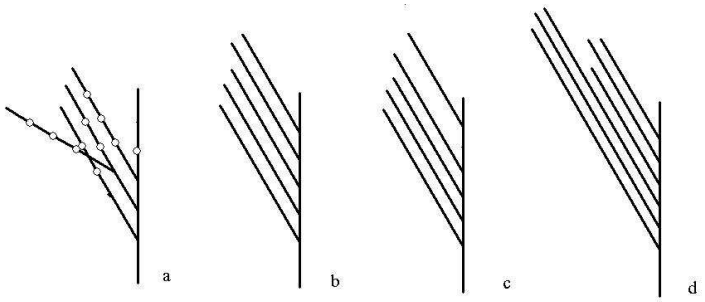

FIGURE 19. The final (stationary) form of the plant for different space steps: for each figure, the step is half of the previous one.

4.3. Graphics. In the graphical representation of the numerical results we will use the following notations and assumptions:

- Branches are represented as black or coloured straight intervals. If a branch grows, then it is shown with brown, as are all preceding branches where the convective flow is nonzero. All other branches are shown with green.

- The angles of the branches with respect to the vertical direction are imposed for the convenience of the graphical representation. It is not determined as a solution of the problem. The starting branch is always vertical. In the 2D simulations the second generation of branches is oriented 15 degrees counterclockwise. The third generation 15 degrees with respect to the parent branches of the second generation, and so on. In the 3D simulations branches have a prescribed spatial orientation.

- The critical values of the concentrations A and K are represented in the coloured representation by blue and yellow points. Where they meet, a new bud grows.

- The total length is the sum of the lengths of all branches.

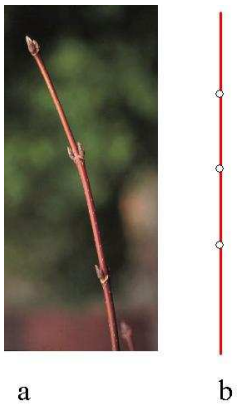

FIGURE 20. A branch with buds: a) real, b) numerical.

4.4. Apical domination. In this section we apply the model described above to study apical domination. This is a well known phenomenon in plant biology which can be described briefly as follows. Growth of a branch can be accompanied by formation of lateral buds (Figure 20). However these buds will not develop while the main branch continues to grow. If the main branch stops growing, then the lateral buds develop into new branches.

It is known that formation of new buds is initiated by the plant hormone cytokinin in the presence of small quantities of auxin ([**11**], page 125). In the framework of our model, we say that a new bud appears if the concentrations of the two hormones have certain values, $A = A_b, K = K_b$. Here A corresponds to auxin, K to cytokinin.

Formation of a new bud, as well as of other plant organs, is accompanied by production of auxin. Therefore, if for some $x = x_0$ and $t = t_0$ the branching condition (4.9) is satisfied, and a new bud appears, then other buds will not appear in the vicinity of the first one, at least for a while. Indeed, production of A during the bud formation changes its concentration, and condition (4.9) will no longer be satisfied.

We should remark here that the role of auxin in suppressing the formation and development of other is not quite clear. It is transported within the phloem only in the direction of the root. On the other hand, there are experiments showing that a

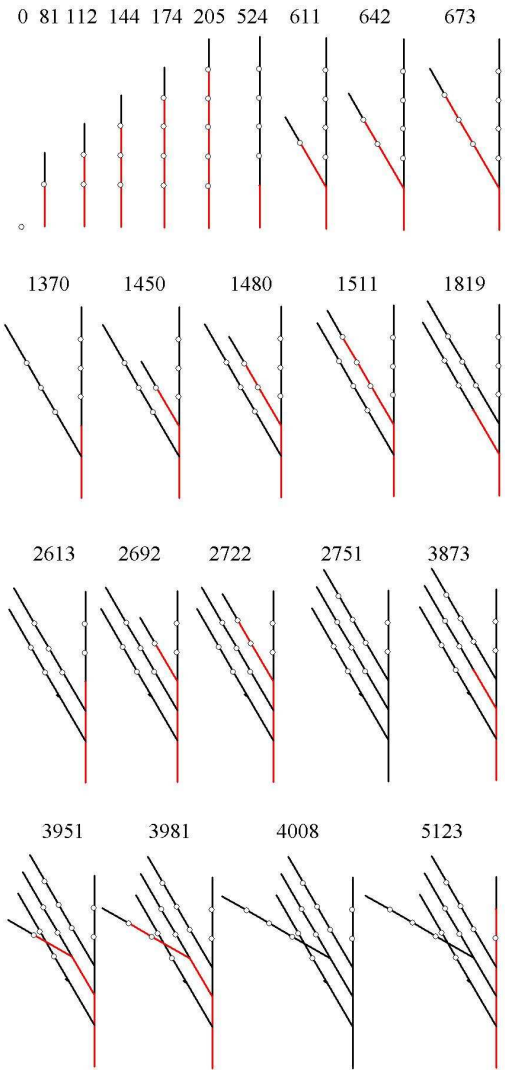

FIGURE 21. Time evolution of the plant. The figure shows the moments in time when new buds or branches appear. The route of nutrients is shown in red.

growing branch can suppress not only growth of lateral buds on the same branch but also those of neighboring branches ([**11**], page 263). This means that the domination can act not only in the direction from the apex to the root but also from the root to the apex. Thus, it is not only auxin that participates in the apical domination but probably also ethylene or some other hormone ([**11**], page 126) that can be produced with the help of auxin and for which transport is not directed. To simplify the

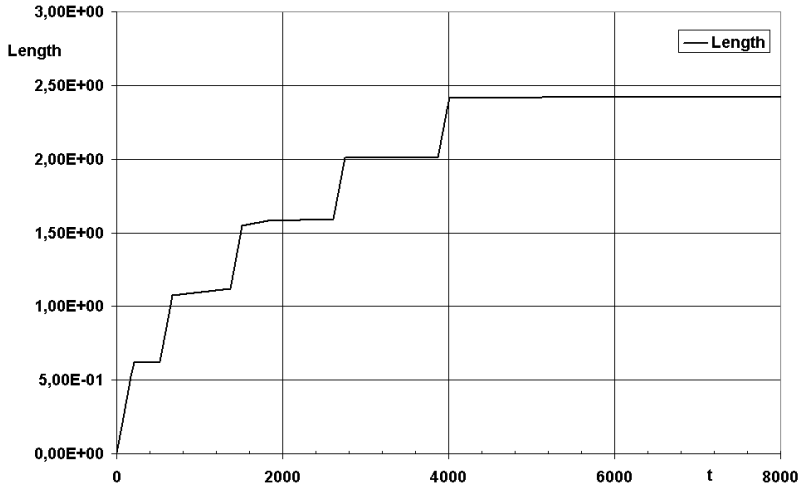

FIGURE 22. Total length as a function of time for the same simulations.

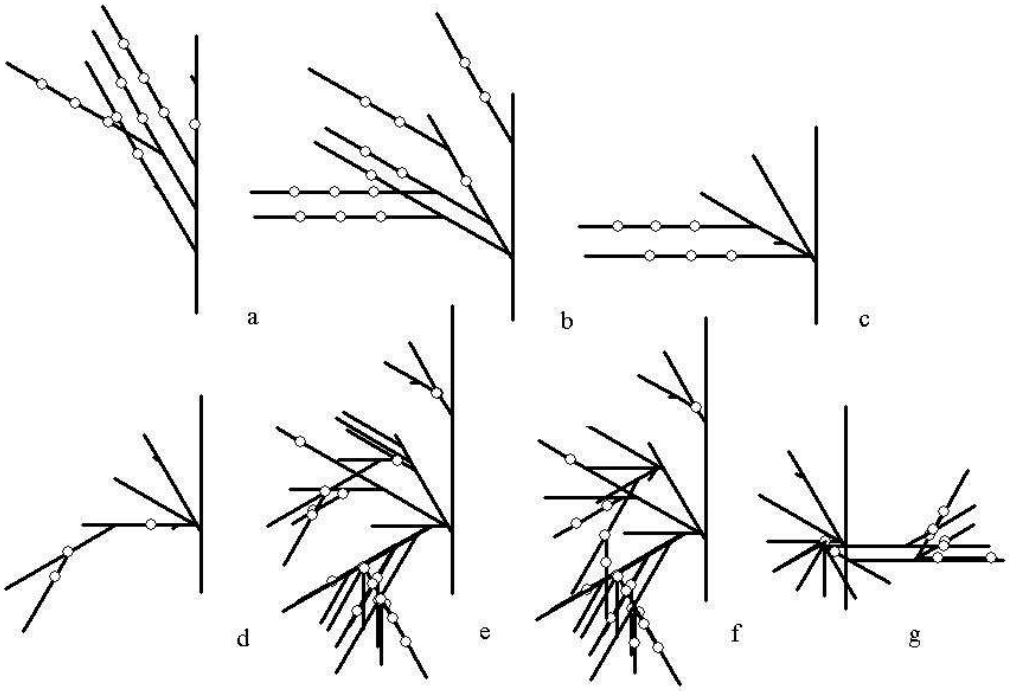

FIGURE 23. The final form of the plant for different initial values of R: a) 0.12; b) 0.13; c) 0.135; d) 0.144; e) 0.1445; f) 0.145; e) 0.15.

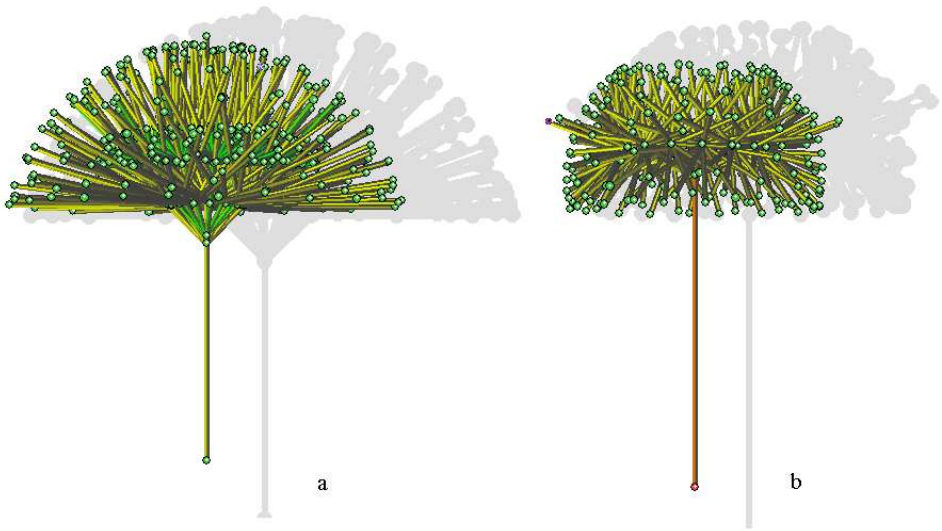

FIGURE 24. Examples of growing plants

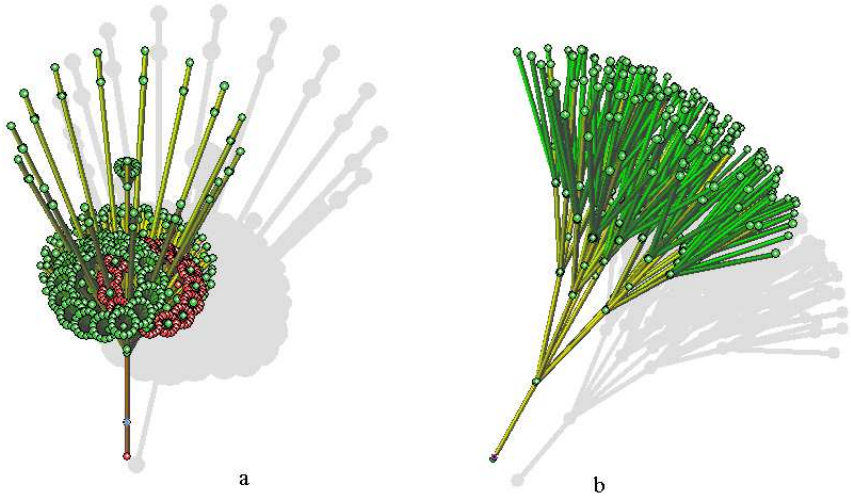

FIGURE 25. Brown branches are growing, green branches do not grow.

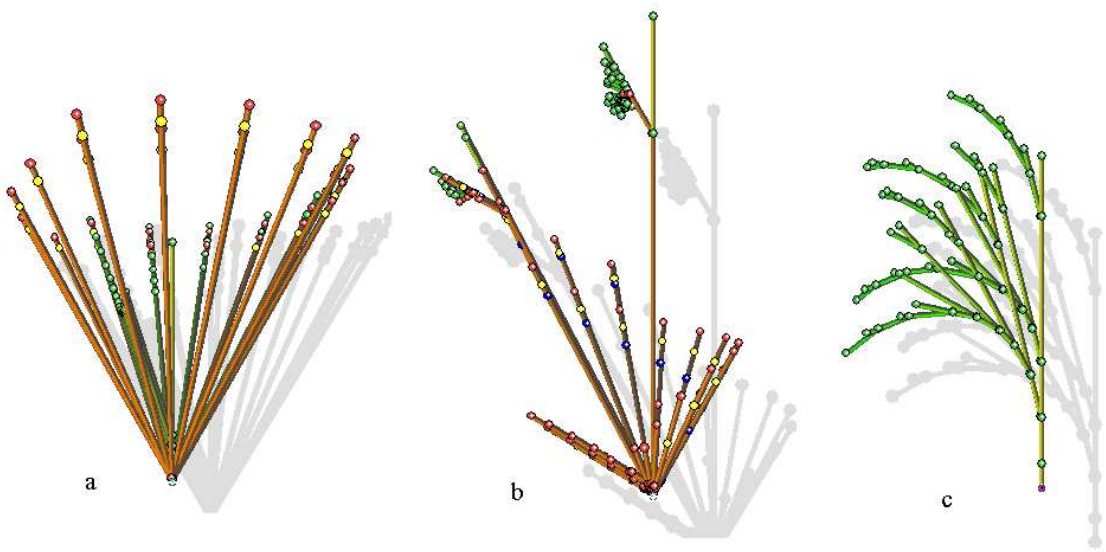

FIGURE 26. Blue and yellow points correspond to the critical concentrations of the hormones. Where they coincide, a new bud appears.

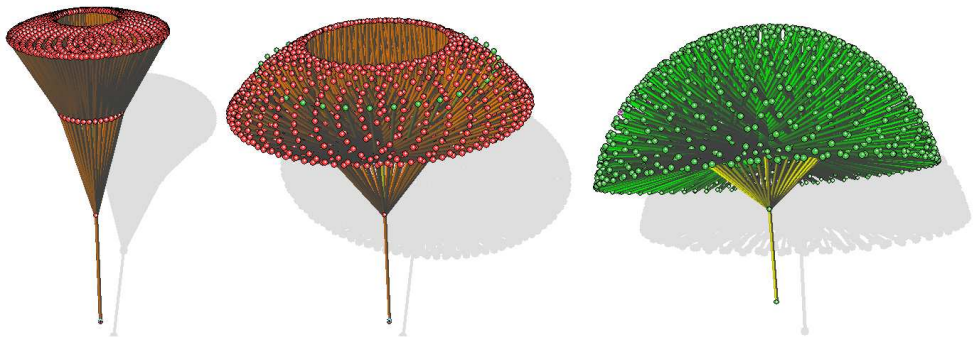

FIGURE 27. Examples of growing plants.

situation, we do not distinguish between auxin and ethylene, and model them with the variable A without the assumption that its transport is directed.

At the first stage of modelling, we observe the growth of the principal branch and formation of new buds. The distance between them is approximately the same (Figure 21). We emphasize that this distance is not prescribed. A new bud appears when condition (4.9) is satisfied.

These buds may not develop into new branches while the principal branch continues to grow. To study this question, we recall first some experimental observations and conclusions ([**11**], page 263). Auxin is produced in the apex of the growing branch. However, its direct implication in the apical domination is not confirmed because of the directed transport discussed above but also because its concentration in the sleeping bud is not higher than in the developing bud. On the other hand, the concentration of cytokinin in the sleeping bud is less than in the developing bud. Artificially adding cytokinin to a sleeping bud will initiate its development.

Growth of branches is determined by cell proliferation related to the concentration of kinetin, which is also produced in the growing parts of the plant. Therefore, the variable R in the model, which we call plant growth factor and which determines the proliferation rate, is related to the concentration of kinetin. On the other hand, kinetin belongs to the group of cytokinins, and cytokinin corresponds to the variable K. Hence the question is whether R and K are the same hormone or a group of hormones.

The following argument shows that they may be not exactly the same. For bud formation, the concentration of cytokinin should be sufficiently high. If it also plays the role of the plant growth factor R, then it would immediately start the bud development and growth of a new branch. Indeed, if its concentration is sufficient for cell proliferation in the case of bud formation it would also be sufficient for cell proliferation for growth. Since it does not always happen, we conclude that the plant growth factor R, though it may be strongly related to kinetin, should not be identified with cytokinin.

Thus, when a new bud is formed, the concentration of cytokinin K is sufficiently high. The concentration of nutrient C in the bud is even greater than in the apex since the nutrients come from the root. Hence the only reason that the bud may not grow is related to the plant growth factor R. We recall that this variable is defined only in the primary or secondary meristem, that is at the upper end of the growing branch or at the new buds. Unlike the variables C, A, and K, which are defined at all points of the interval and whose values in the bud are the same as at the corresponding point of the branch, the value of R in a newly formed branch should be prescribed. If this initial value is sufficiently small then the bud will not develop. If it is high, the new branch starts growing right away and apical domination does not occur.

The initial value of R in a newly formed bud can depend on the concentration K at this point of the branch or on other factors. At this stage of the modelling we consider it to be a parameter of the problem that we can prescribe and vary.

In the simulation shown in Figure 21, the initial value of R in all buds is 0.01. The same figure shows further evolution of the plant. The new buds begin to develop into branches when the concentration of the plant growth factor R is sufficiently high. Its concentration is described by the equation in (4.5). The rate of production of R

depends on the concentration of nutrients C. Since they are supplied from the root, their concentration is highest in the lowest bud. It begins to develop first. Its growth is also accompanied by formation of buds. Then the second-lowest bud gives a new branch, and then the third-lowest. We note that the first lateral branch yields a small branch of the third generation, the second branch yields a big branch of the third generation, and the fifth bud on the main branch also develops into a small branch.

The evolution of the total length over time is shown in Figure 22. Each step of this function corresponds to the appearance of a new branch. The time interval between new branches increases. The dependence of the total length on time is similar to that of the 1D case without branching (Figure 3).

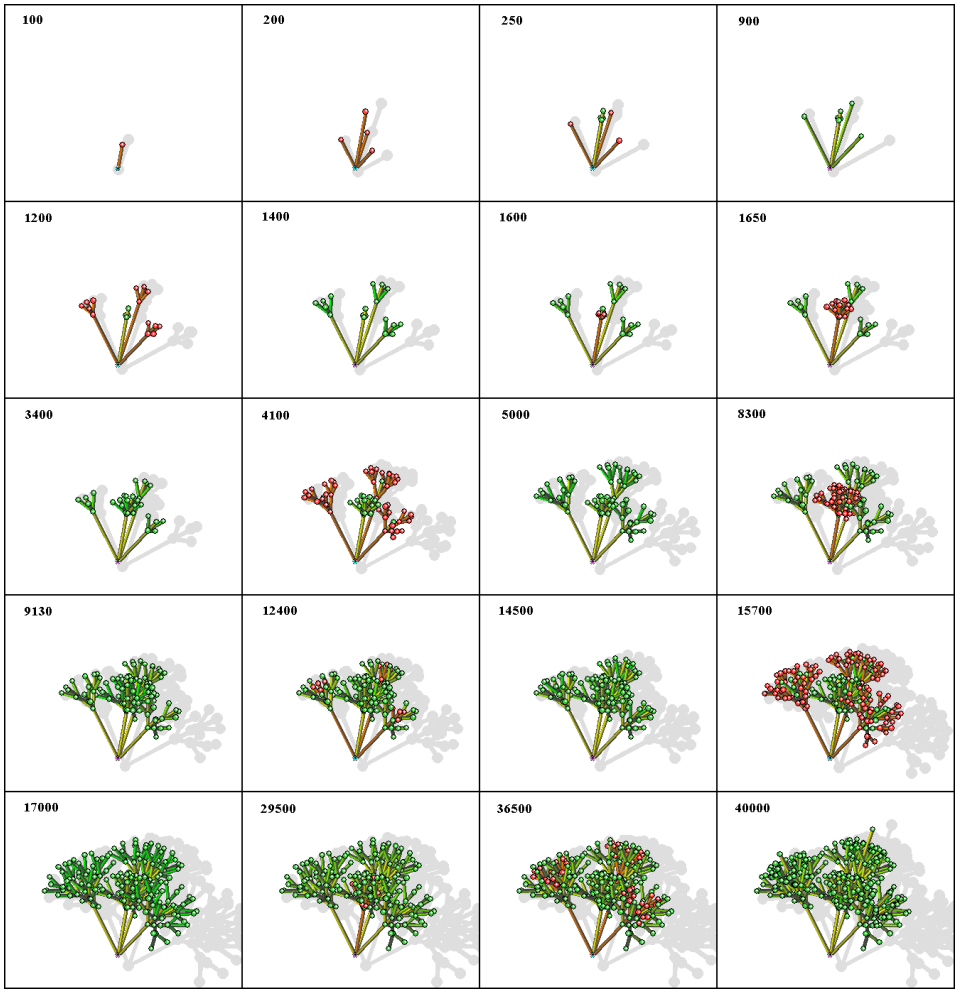

FIGURE 28. Time evolution in the case of three branches growing from the same bud.

4.5. Plant architecture. In this section we vary the parameters of the problem and present the numerical results. Figure 23 shows the evolution of the final form of the plant for different values of the initial concentration R_0 of the GM-factor. For R_0 sufficiently high, apical domination does not occur though there may exist some buds in a latent state.

Several examples of emerging plant forms are shown in Figures 24 - 27. We note that, in a real plant, two or three buds can appear simultaneously at the same place of the branch. This means that there can be several new branches starting from the same point. Figure 28 shows the time evolution of the plant with three branches starting from the same place.

We also consider the case where the value R_0 is not given *a priori* for a new bud but taken equal to its value in the apical meristem (Figure 26). We do not know whether this situation is realistic from the biological point of view but we cannot exclude existence of communication between the apical meristem and the lateral buds.

5. Discussion

5.1. Why are plants not eternal? Unlike animal cells, plant cells are not limited in the number of their divisions. Therefore, they can theoretically divide an infinite number of times, and plants can have an infinite lifespan. Practically, however, this is not the case.

From the standpoint of the modelling presented in this work, plant death corresponds to a stable stationary solution. After reaching this state the plant will not grow any longer, and the meristem cells will not divide.

The time of convergence to a stationary solution can strongly depend on parameters but depends weakly on the initial conditions. If we relate the parameters to the plant type, then this means that each plant species has its lifespan. But this also depends on the external conditions. If the concentration of available nutrients decreases (the boundary condition for C at $x = 0$), then the final length and the lifespan also decrease.

Thus we come to the question of whether the solution of the evolution problem will necessarily converge to a stationary solution. In the numerical simulations for the one-dimensional case without branching, convergence to a stationary solution is always observed. Since in this case the stationary solution is very simple (C is a linear function of x) we can easily verify that it is indeed a stationary solution.

It is more difficult to verify in the one-dimensional case with branching. For relatively simple plant structures we observe convergence to stationary solutions. We do not know whether the convergence always occurs for plants with complex structures.

The question about convergence to stationary solutions becomes even more complex in the two-dimensional case. When the plant stops growing, another growth period can begin some time later. Since the duration of the rest state can be very long, as in the one-dimensional case without branching, the computational time does not allow us to verify whether the solution of the evolution problem will converge to a stationary solution.

From the biological point of view, plant death probably occurs as a result of gradual changes of the morphogenetic fields [**3**] that make the concentration of growth and mitosis factors reach their equilibrium. This hypothesis is in agreement with the results of the numerical simulations.

5.2. Emergence of forms. One of the basic questions of mathematical biology is about the mechanism of biological pattern formation. The oldest and the most well-known mechanism is given by Turing structures [**22**]. They imply the existence of a short range activation and a long range inhibition. From the mathematical point of view it should be a system of two or more reaction-diffusion equations

$$\frac{\partial u}{\partial t} = d_1 \frac{\partial^2 u}{\partial x^2} + F_1(u, v), \quad \frac{\partial v}{\partial t} = d_2 \frac{\partial^2 v}{\partial x^2} + F_2(u, v) \tag{5.1}$$

with very different diffusion coefficients d_1 and d_2 and with some additional conditions on the nonlinearities F_1 and F_2. This system is considered in the interval $0 \le x \le L$

with, for example, periodic or no-flux boundary conditions. Let us assume that there exists a homogeneous in space equilibrium, that is the values u_0 and v_0 of the concentrations such that

$$F_1(u_0, v_0) = F_2(u_0, v_0) = 0.$$

Then it is a stationary solution of the kinetic system of equations

$$\frac{du}{dt} = F_1(u, v), \quad \frac{dv}{dt} = F_2(u, v). \tag{5.2}$$

It is possible that the homogeneous stationary solution is stable with respect to system (5.2) and unstable with respect to system (5.1). In this case, the solution of the reaction-diffusion system of equations can converge to another stationary solution, which is not homogeneous in space. This solution is called the Turing or dissipative structure.

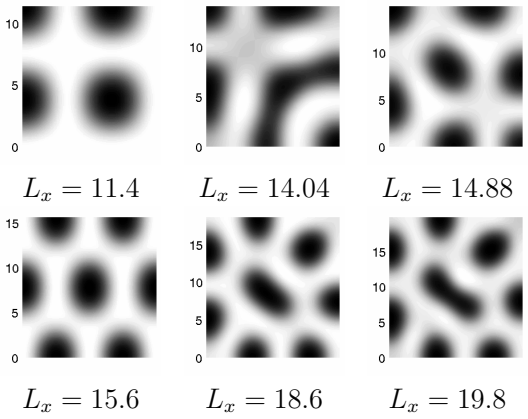

FIGURE 29. Example of Turing structures in square domains (from [**7**]).

Linear stability analysis of the homogeneous stationary solution gives explicit conditions of the appearance of the Turing structure. It can be verified that the solution $u = u_0, v = v_0$ loses its stability if the length L of the interval is sufficiently large. For small L the solution is stable. This situation suggests some biological interpretations. One of them is related to differentiation of cells in the embryo, where all cells are initially identical. When the embryo becomes sufficiently large, the instability described above produces a nonhomogeneous distribution of some chemical species that lead to expression of different genes in different parts of the embryo. Turing structures are also used to describe skin patterns for some animals [**17**], patterns on sea shells [**16**], and some other biological phenomena. In some cases the results of the modelling are amazingly close to real biological patterns.

These models are phenomenological. They do not describe real biological mechanisms, or at least the activator and the inhibitor required for emergence of Turing structures are not known ([**23**], page 347). Moreover, biological systems are very complex. In many regulatory networks, dozens of proteins are directly involved, and

hundreds are involved indirectly. It is not clear whether they can be described by simple reaction-diffusion systems with two or three variables.

Among other mechanisms of patterns formation we will mention mechano-chemical phenomena [**17**] and the theory of morphogenetic gradients [**23**].

What is the mechanism of pattern formation observed in this work? We will discuss two different cases: appearance of branches in the one-dimensional simulations with branching and emergence of structures in the two-dimensional simulations. In both cases there is an initial asymmetry introduced in the model. We suppose that the root and the meristem are already formed. We should note that the apical-basal asymmetry exists in plants from the very early stages of development of the embryo. Therefore, the mathematical idealization of the question about cell differentiation in the embryo formed from a number of identical cells is not applicable here. The initial embryo cell (zygote) is not itself symmetric. When it divides into two cells, one of them gives the basal part of the plant (root), another one the apical part (shoot).

FIGURE 30. Growth of leaf primordia - 1.

Modelling of the transition from the embryo to the adult plant is a subject for future works. In this work we study the case where the meristem is already formed. Moreover, the plant is supposed to be sufficiently large such that the mersitem is small with respect to the whole plant.

To describe appearance of new branches we suppose, in accordance with plant biology, that two hormones, auxin and cytokinin are produced in the apical meristem. They are transported from the meristem along the branch. When their concentrations take on certain values, a new bud appears accompanied by production of additional quantities of the hormones. Therefore, their concentrations change, the conditions for a new bud to appear are no longer satisfied, and there are no other buds in the vicinity of the first one. After some time another bud can appear at some distance from the first one.

This mechanism is very different in comparison with Turing structures. First, the two hormones do not correspond to activator and inhibitor. Moreover, they are produced at the very end of the growing shoot and not all along its length. Therefore, their interaction cannot result in emergence of spatial structures. The branching mechanism is more closely related to the theory of morphogenetic gradients.

There are no hormones in the two-dimensional model. The mechanism of pattern formation is different. We recall that when the concentration of nutrients becomes sufficiently low, the GM-factor is not produced any longer, its concentration decreases,

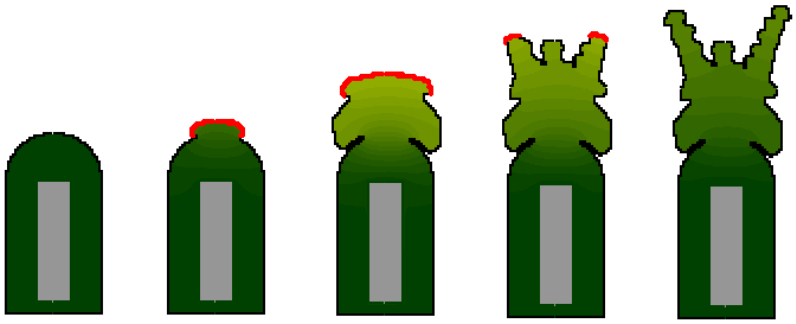

FIGURE 31. Growth of leaf primordia - 2.

and growth stops. Patterns in the 2D simulations appear when the concentration of nutrients is close to its critical value. It is not sufficient to support uniform growth. It stops at some parts of the boundary and continues at some other parts.

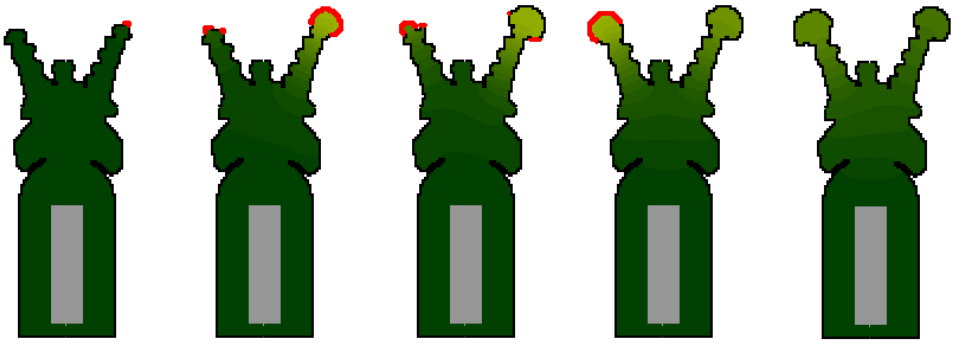

FIGURE 32. Growth of leaf primordia - 3.

To describe this mechanism more precisely, consider the plant in the dormant state just before the new growth period begins. The plant has accumulated nutrients, and the concentration of the GM-factor in the meristem is already sufficiently high. If it increases slightly more, its self-accelerating production will begin, its concentration will rapidly increase, and the plant will start growing. Suppose that there is a small perturbation of the GM-factor concentration at some part of the boundary where it is greater than at surrounding parts. Then self-accelerating production of the GM-factor will begin at this part of the boundary, its concentration will rapidly increase, the plant starts growing, and the concentration of nutrients rapidly decreases. Therefore the concentration of the GM-factor will decrease at the neighboring parts of the boundary and growth there will not take place. At the same time, it will continue where it has already started because the concentration of the GM factor there is high.

The right-hand side of the equation

$$h\frac{dR}{dt} = Cg(R) - \sigma R \tag{5.3}$$

is positive even if C decreases (since g has a sharp maximum), and the production of R continues. We note that this description is close to that of appearance of leaf primordia in the apex of Arabidopsis (see [**20**]). There, auxin plays the role of the GM-factor. The mechanism of pattern formation has some similarity with that for crystallization, in which a local increase of the speed of the moving boundary changes the temperature distribution that results in further increase of the perturbation.

Figures 30 and 31-32 show an example of pattern formation that can be interpreted as growth of leaf primordia.

5.3. Apical domination. Apical domination is a well-known phenomenon in plant biology in which a growing shoot suppresses growth of other branches. The explanation of this effect is usually related to production of auxin in the apex of the growing plant. However, the exact mechanism of apical domination is not known and the role of auxin is not precisely specified. Firstly, auxin is transported from the apex in the direction of the root along the phloem due to its polar transport. However, it is known that apical domination can act not only on the dormant bud of the growing shoot but also on the apex of other branches (see [**11**], page 263). Therefore, there are also some other biological products involved in apical domination. For example, it can be ethylene produced with the help of auxin. The transport of ethylene is not polar, so it can be transmitted to the apex of a neighboring branch. This is why we do not distinguish auxin from ethylene and do not take into account its polar transport when we study apical domination.

The second question about the role of auxin in apical domination is related to experimental results that show that adding some other hormones to a dormant bud (for example cytokinin) will "wake it up" resulting in the growth of a new branch. Therefore it is not only the concentration of auxin that is involved in this process.

There are four variables in our model: concentrations of auxin, cytokinin, mitosis and growth factor, and nutrients. Analysis of the numerical simulations show that an interaction of all these variables can result in apical domination. Concentrations of auxin and cytokinin determine the appearance of a new bud. However, it may remain dormant, which shows that conditions for the appearance of a bud and for its growth are different. We consider a bud as a small branch with the same conditions for growth as those of actual branches. These conditions are determined by the concentrations of nutrients and of GM-factor. If we add GM-factor to a dormant bud, it will start growing. GM-factor can be produced by the bud itself. The rate of its production is determined by its initial concentration R_0 in the bud and by the concentration of nutrients. If the concentration of nutrients is low, then GM-factor is not produced and the bud remains dormant. The growing shoot consumes nutrients and, consequently, influences the production of GM-factor in the buds. If the growing shoot is cut off, there are more nutrients for the buds, the production of GM-factor increases, and the buds start growing.

The initial concentration R_0 of GM-factor in the bud is a parameter that determines whether apical domination occurs. If this concentration is low, then the bud needs more time and more nutrients to produce a sufficient amount of GM-factor. If R_0 is sufficiently large, then the bud can start growing immediately after its appearance, and apical domination will not occur.

5.4. Gene expression. Modern plant biology studies gene expressions in relation with formation of plant organs. We can mention, for example, the genes Clavata 1, Clavata 3, and Wuschel that determine localization of the apical meristem ([**2**], page 1252). Genes Apetala2, Apetala3, and Agamous are involved in the regulation of flower development in Arabidopsis ([**1**], page 1118; see also the review article [**14**]). There are many studies of interactions between plant hormones and gene expressions (see, e.g., [**15**]). It is not yet quite clear how this information can be introduced in mathematical models because it usually describes only a part of regulatory networks and, consequently, does not allow suggestion of a closed model. On the other hand, complete regulatory networks (even if we suppose that some of them will be fully described), will be too complicated to use in the modelling. This is the principal restriction in the development of mathematical biology.

5.5. Biological diversity and structural stability. How should we interpret the existence of many different biological forms (different biological species) from the point of view of mathematical modelling? Why are all individuals of the same species different but also similar to each other?

We will try to give some answers to these questions in the framework of the modelling presented in this work. The first fundamental property of the models considered above is that they possess continuous families of stationary solutions for the same values of the parameters. In the 1D case it can be all intervals with length greater than the minimal one. In the 2D case it can be practically all plane forms with some nonrestrictive conditions on the curvature (see Annexe 3). We recall that the genetic information that determines the plant type is associate in our model with the values of parameters. If the set of stationary solutions for the same values of parameters would be discrete, then the plants of the same species would have a discrete set of final forms and sizes. All fir-trees would be split into subclasses with exactly the same number and length of branches and needles. This seems impossible. The differences in the initial conditions and external conditions result in differences among individuals of the same species. This is possibly due to the fact that all solutions are possible.

What happens if we change the parameters of the model? Its second fundamental property is that stationary solutions exist for all physically realistic values of parameters. Therefore, not only the individuals of a given species can have an arbitrary form but individuals of any species can have any possible form. This is why there are so many different forms and different species. Of course, this is only a theoretical possibility. The existence of stationary solutions does not necessary mean that the solution of the evolution problem with some specific initial condition will converge to them.

If we slightly change the parameters of the model, the initial condition or the external conditions (that is the boundary conditions in the model), or the space and time steps in numerical simulations, we never obtain the convergence to exactly the same stationary solutions. We can expect that if the difference in parameters is small, the solutions will be close to each other. It appears, however, that this is not necessarily so. In some cases, the solutions are close to each other, while in some other cases they can be essentially different. The former case corresponds to individuals of the same species, the latter, to transition to other species.

We come now to the question about the structural stability of solutions: if the values of parameters approach each other, will the solutions also converge to each other? The results of the numerical simulations show that this is probably not the case. When we decrease the time and space steps we do not obtain the convergence of solutions. At first glance this contradicts the unwritten convention of numerical modelling: solutions must converge. However, there is no contradiction. The usual expectation that solutions converge concerns a fixed and finite time interval. This rule is not applicable to the longtime behavior. What does longtime behavior mean? Of course, numerical simulations are always carried out on a finite time interval. To explain this, consider a typical situation in the theory of dynamical systems in which a stationary solution can have a stable manifold along which solutions of the evolution problem approach the stationary solution as time increases, and unstable manifold along which solutions of the evolution problem diverge from the stationary solution. If the initial condition is close to the stable manifold but it is not located exactly on it, then in the beginning the solution of the evolution problem will approach the stationary solution, but after some time diverge from it. For two different but close initial conditions, the solutions of the evolution problem will first approach each other, but then at the second stage the difference between them will increase and after some time they can become completely different.

How is this description related to the modelling of plant growth? The solution of the evolution problem approaches some unstable stationary solution along its stable manifolds and then moves away from it along the unstable manifold (see the next section for more details). Small perturbations grow exponentially, and convergence of solutions, when we decrease the time and space steps, does not take place.

Thus, solutions are not structurally stable in the usual sense. However, they can be structurally stable in some averaged sense: changing the parameters, we can observe similar structures with the same characteristic dimensions, though different in small details. The conclusion that biological forms can be structurally stable in some averaged sense is in agreement with the fact that individuals from the same species, though different from each other, still have many features in common. On the other hand, in some cases structural stability does not take place even in average. The presence of stable and unstable manifolds can result in essential difference of solutions with close initial conditions. This situation can be considered as transition to new biological species.

5.6. Nonlinear dynamics. The typical behavior of the evolution problem in the 1D case consists in the alternation of growth periods during which the interface moves (i.e., the length of the interval grows), and of rest periods where it is unmovable. After several such cycles the solution converges to a stationary solution. This stationary solution is stable, and the oscillations occur far from it. So the appearance of the oscillations is not related to a Hopf bifurcation, in which a stationary solution loses its stability, resulting in the bifurcation of a limit cycle near it.

To explain this dynamic we should remark that the problem possesses two continuous families of stationary solutions. We will denote them by $v_s(L)$ and $v_u(L)$. Here the subscript s corresponds to stable solutions, u to unstable solutions, and L to the length of the interval; in both cases solutions exist for all L (L should be sufficiently large in the case of stable solutions). Stationary solutions are in fact couples $(C(x), R)$, where $C(x)$ is the concentration distribution in the interval $[0, L]$, and R is the value of the concentration of the growth and mitosis factor at $x = L$. For stable stationary solutions $C(x)$ is a linear function, and R is some positive constant, for unstable solutions; $C(x)$ is constant, $R = 0$.

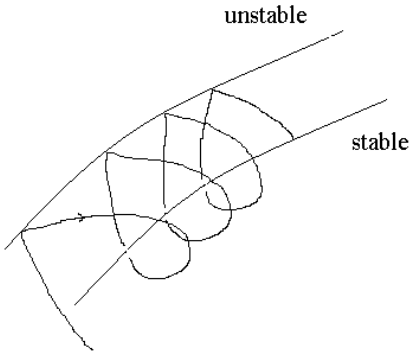

FIGURE 33. Schematic representation of solutions of the 1D evolution problem

Stability of stationary solutions is determined by the stability of R considered as a stationary solution of equation (5.3). If $C = C(L)$ in this equation is fixed, then it can have from one to three stationary solutions (for functions $g(R)$ considered in this work). For small C, the right-hand side of this equation is negative, and $R = 0$ is its stable stationary solution, for C close to 1, it is unstable.

These properties of the problem explain why solutions $v_u(L)$ are unstable or, more precisely, have stable and unstable manifolds. In the evolution problem, there is a coupling between the concentration distribution inside the interval, the value R, and

the growth of the interval length. The value of C at $x = L$ is a function of time. During growth periods it becomes small because nutrients are consumed. Therefore, $R = 0$ becomes stable with respect to equation (5.3). The solution of the evolution problem approaches one of the stationary solutions from $v_u(L)$. During rest periods, the concentration $C(x,t)$ gradually increases, approaching 1 everywhere inside the interval. When $C(L,t)$ becomes sufficiently large, $R = 0$ becomes unstable with respect to equation (5.3). The value of R grows, and when it is sufficiently large, a new growth period begins.

This is the mechanism of oscillations in the 1D problem without branching. It is shown schematically in Figure 37 with two families of stationary solutions and a trajectory corresponding to the solution of the evolution problem. Similar behavior is observed for some crystallization problems [**6**].

In the 1D case with branching the qualitative behavior is the same. It becomes more complex because of the interaction of several growing branches. It is even more complex in the 2D case where each point (numerical cell) at the boundary represents an oscillator described above. These oscillators are coupled through the external field (concentration of nutrients inside the domain). There are clearly two characteristic time scales for the 2D problem. One of them is related to high frequency oscillations which are probably local, where a relatively small portion of the boundary cells are involved. Another time scale is related to the alternation of growth and rest periods, where all boundary cells are in the rest state (see Figure 9). We should note that stable and unstable stationary solutions exist in the 2D case for practically all plane domains (with some weak restrictions on the curvature - see Annexe 3). This explains the wide variety and complexity of emerging forms.

5.7. Evolution of species. In Darwin's theory of the evolution of species, intraspecific competition and random mutations can result in the emergence of new biological species. In spite of numerous discussions about it, this theory remains the only explanation of the emergence of species. There are mathematical models and results, which describe this phenomenon and seem to be in agreement with Darwin's theory (see [**8**] and the references therein).

The modelling presented in this work suggests another mechanism of the appearance of biological species in the process of evolution. To describe it, we summarize the mechanism of plant growth described above. There are two families of stationary solutions, stable and unstable. The solution of the evolution problem approaches an unstable solution and then diverges from it. After that, it can approach another unstable stationary solution, and so on. After several such cycles it approaches a stable stationary solutions and does not change any longer. The number of cycles depends on the values of the parameters. If we gradually vary the parameters, the corresponding stationary solutions can also be close to each other, in the case of structural stability, or can be essentially different, otherwise.

We now consider this behavior in the evolution context. For this, we need to establish a connection between individuals of consecutive generations. Suppose that a newly born individual of the n-th generation is characterized by a set of parameters

P_n. After some time it becomes adult and produces an individual of the $(n+1)$-th generations with parameters P_{n+1}. We can assume that under constant external conditions, the properties of the young individual uniquely define the adult individual and, consequently, the young individual of the next generation (asexual reproduction). Then $P_{n+1} = F(P_n)$, where F is some given function. Thus, we have a relation between the parameters characterizing consecutive generations of individuals.

If $P_{n+1} = P_n$, then it is a stationary point of the mapping $F(P)$, that is a point P_s for which $P_s = F(P_s)$. Stationary points can be stable or unstable depending on the eigenvalues of the matrix $F'(P_s)$. In the case of a stable stationary point, small perturbations decay, and P_n will remain in a neighborhood of P_s for all n. In the case of an unstable point, P_n can go away from it as n increases.

Thus, there are two possible situations. If P_n is in a neighborhood of a stable stationary point, then these species will not evolve any longer. This is a final form of evolution. If P_n is in a neighborhood of an unstable stationary point or it is far from stationary points, then it will change from one generation to another. This change is not related to random perturbations. It is a deterministic change in a certain direction determined by properties of the function F.

The modelling presented in this work allows the description of the transition from young to adult individuals. The transition to young individuals of the next generation can be accompanied by a gradual change of parameters from one generation to another. Therefore, we have a sequence of 1D or 2D problems considered in Sections 2-4, which differ by the values of parameters. As it is discussed above, solutions may not be structurally stable. Therefore, evolution of a group of individuals can be described as follows. During a number of generations, they gradually change remaining similar to each other. At some point, there is a fast transition to individuals with another phenotype. After that, there can be another period of gradual changes, and possibly another fast transition. Such evolution will continue until a final stage where the parameters P_n approach a stable stationary point of the mapping $F(P)$.

We finally note that two subgroups of the same species separated from each other can originate, in the process of evolution, two different species. This cannot be explained by intra-specific competition but can probably be explained in the framework of the mechanism described in this section.

6. Annexe 1. Numerical algorithm: 1D with branching

In this section we discuss the numerical algorithm for the one-dimensional problem with branching. The model is based on the reaction-diffusion equations, which can be considered in the following form:

$$\frac{\partial \varphi}{\partial t} + u\frac{\partial \varphi}{\partial x} = d\frac{\partial^2 \varphi}{\partial x^2} - \mu\varphi, \tag{6.1}$$

where φ corresponds to the unknown variable (e.g. C, K), x is the space variable defined on each particular branch. Let us introduce a finite-difference mesh along any branch with the nodal coordinates x_i $(i = 1, \dots, I)$ (Figure 34a).

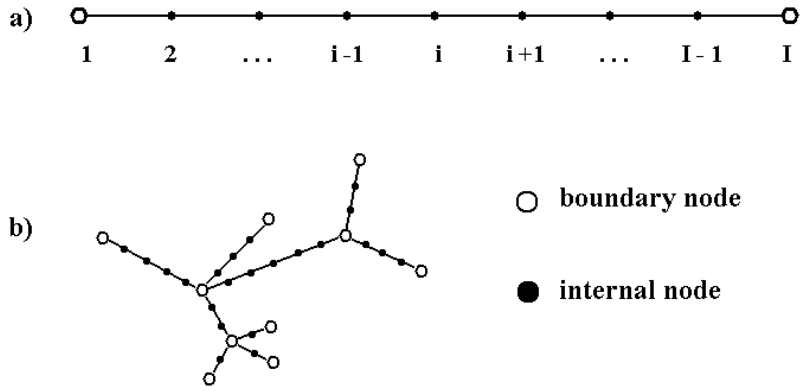

FIGURE 34. Numerical mesh with branching

Let the nodes x_i be located uniformly with distance dx between them. We will denote the values of φ in the nodes by φ_i. Consider an explicit upwind approximation for equation (6.1) first in the interior nodes $(i = 2, \dots, I-1)$

$$\frac{\varphi_i^n - \varphi_i^{n-1}}{dt} + (|u| + u)\frac{\varphi_{i+1}^n - \varphi_i^n}{2dx} + (|u| - u)\frac{\varphi_{i-1}^n - \varphi_i^n}{2dx}$$

$$= d\frac{\varphi_{i+1}^n - 2\varphi_i^n + \varphi_{i-1}^n}{dx^2} - \mu\varphi_i^n, \tag{6.2}$$

where dt is the time step. The superscript n corresponds to the time step. To simplify the notations, in what follows we will omit n, that is, we will write φ_i instead of φ_i^n. and will keep the notation φ_i^{n-1}. Let us write equation (6.2) in the form

$$a_i\varphi_{i-1} - c_i\varphi_i + b_i\varphi_{i+1} = -f_i, \quad i = 2, \dots, I-1, \tag{6.3}$$

where

$$a_i = \frac{|u| - u}{2dx} + \frac{d}{dx^2}, \quad b_i = \frac{|u| + u}{2dx} + \frac{d}{dx^2},$$

$$c_i = \frac{1}{dt} + \frac{|u|}{dx} + \frac{2d}{dx^2} + \mu, \quad f_i = \frac{\varphi_i^{n-1}}{dt}. \tag{6.4}$$

Consider now the approximation of the boundary conditions. If the ends of the branch correspond to the root ($x = 0$) or to the growing part (Figure 33a), then the approximation of the boundary conditions here yields the expressions:

$$-c_1\varphi_1 + b_1\varphi_2 = -f_1, \tag{6.5}$$

and

$$a_I\varphi_{I-1} - c_I\varphi_I = -f_I. \tag{6.6}$$

Specific expressions for $a_1, b_1, \ldots, f_I$ in the case of some particular boundary conditions can be done in the same way.

In the case of the growth of a single branch, the numerical scheme is completely described by system (6.3), (6.5), and (6.6). The matrix of this system is tri-diagonal:

$$\begin{pmatrix} -c_1 & b_1 & 0 & 0 & 0 & 0 & 0 & \ldots & 0 \\ a_2 & -c_2 & b_2 & 0 & 0 & 0 & 0 & \ldots & 0 \\ \ldots & & & & & & & & \\ 0 & \ldots & 0 & a_i & -c_i & b_i & 0 & \ldots & 0 \\ \ldots & & & & & & & & \\ 0 & \ldots & 0 & 0 & 0 & 0 & a_{I-1} & -c_{I-1} & b_{I-1} \\ 0 & \ldots & 0 & 0 & 0 & 0 & 0 & a_I & -c_I \end{pmatrix}. \tag{6.7}$$

To solve a linear system with a tri-diagonal matrix (6.7) we can use the Thomas algorithm.

The situation is more difficult if there are several branches. Moreover, the tree can have an arbitrary structure (see, e.g., Figure 34b). There are nodes from which several branches end or begin. Such nodes will also be called boundary nodes. Each of them will be numbered, and the value of φ at the k-th node is denoted by φ_k. The boundary conditions in the conventional sense are not imposed in such nodes. Instead, we should take into account conservation of species and fluxes.

For certainty, let there exist J branches leaving the boundary node k. Then $\varphi_{j,1} = \varphi_k$ at $j = 1, \ldots, J$. The values of φ at the second node of each branch will be denoted by $\varphi_{j,2}$, at the third $\varphi_{j,3}$, and so on. Then the conservation of φ at the node k can be written as follows:

$$\sum_{j=1}^{J} \left(d\frac{\varphi_{j,2} - \varphi_k}{dx} - \mu\frac{dx}{2}\varphi_k - \frac{dx(\varphi_k - \varphi_k^{n-1})}{2dt} - \frac{|u_j| - u_j}{2}(\varphi_k - \varphi_{j,2}) \right) = 0. \tag{6.8}$$

If there are J branches entering the boundary node k, then the finite difference scheme at this node will be:

$$\sum_{j=1}^{J} \left(d\frac{\varphi_{j,I-1} - \varphi_k}{dx} - \mu\frac{dx}{2}\varphi_k - \frac{dx(\varphi_k - \varphi_k^{n-1})}{2dt} - \frac{|u_j| + u_j}{2}(\varphi_k - \varphi_{j,I-1}) \right) = 0. \tag{6.9}$$

If for some of the branches the numeration begins at the node k and for some other it ends there, then the finite difference scheme can be represented as a superposition of (6.8) and (6.9).

To summarize, we recall that, in the internal nodes of the mesh, we use a three-point scheme (6.3). In the boundary nodes, we have expressions (6.8) or (6.9) (see Figure 34b) that include φ_k and the values $\varphi_{j,I-1}$ or $\varphi_{j,2}$ taken at the nodes nearest to the boundary node from the branches connected to this node. Thus we have a completely implicit approximation of our 1D problem.

We describe here the algorithm for the case in which the domain of the computation has several branches arbitrarily connected between each other. Moreover, the number of branches can change during the computation.

The finite difference scheme for the internal nodes of the j-th subsystem has the following form:

$$\begin{cases} -c_1\varphi_{k_1} + b_1\varphi_2 = -f_1 + \text{other terms}, \\ \\ a_i\varphi_{i-1} - c_i\varphi_i + b_i\varphi_{i+1} = -f_i, \quad i = 2, \dots, I-1 \\ \\ a_I\varphi_{k_2} - c_I\varphi_{I-1} = -f_I + \text{other terms}. \end{cases} \tag{6.10}$$

The first and the last equations in system (6.10) are obtained from expressions (6.8) and (6.9) corresponding to k_1-th and k_2-th boundary nodes. The terms corresponding to the j-th branch are written explicitly; for other branches they are included in "other terms".

Instead of the tri-diagonal matrix (6.7) we have here an "almost tri-diagonal" matrix for the j-th branch:

$$\begin{pmatrix} -c_1 & b_1 & 0 & 0 & 0 & 0 & 0 & \dots & 0 & \text{other terms} \\ a_2 & -c_2 & b_2 & 0 & 0 & 0 & 0 & \dots & 0 & \\ \dots & & & & & & & & & \\ 0 & \dots & 0 & a_i & -c_i & b_i & 0 & \dots & 0 & \\ \dots & & & & & & & & & \\ 0 & \dots & 0 & 0 & 0 & 0 & a_{I-1} & -c_{I-1} & b_{I-1} & \\ 0 & \dots & 0 & 0 & 0 & 0 & 0 & a_I & -c_I & \text{other terms} \end{pmatrix}. \tag{6.11}$$

Step 1. Transformation of matrix (6.11) to an "almost two-diagonal" form. Let us write the corresponding system (6.10) in the form

$$\begin{cases} -c_1\varphi_{k_1} + b_1\varphi_2 = -f_1 + \text{other terms}, \\ \\ \beta_i\varphi_{k_1} - \varphi_i + \alpha_i\varphi_{i+1} = -\gamma_i, \quad i = 2, \dots, I-1, \\ \\ a_I\varphi_{k_2} - c_I\varphi_{I-1} = -f_I + \text{other terms}, \end{cases} \tag{6.12}$$

where

$$\alpha_i = \frac{b_i}{c_i - \alpha_{i-1}a_i}, \quad \beta_i = \frac{a_i\beta_i}{c_i - \alpha_{i-1}a_i},$$

$$\gamma_i = \frac{a_i\gamma_{i-1} + f_i}{c_i - \alpha_{i-1}a_i}, \quad i = 3, \dots, I-1 \tag{6.13}$$

and

$$\alpha_2 = \frac{b_2}{c_2}, \quad \beta_2 = \frac{a_2}{c_2}, \quad \gamma_2 = \frac{f_2}{c_2}. \tag{6.14}$$

Thus, matrix (6.11) is reduced to the following one:

$$\begin{pmatrix} -c_1 & b_1 & 0 & 0 & 0 & 0 & 0 & \dots & 0 & \text{other terms} \\ \beta_2 & -1 & \alpha_2 & 0 & 0 & 0 & 0 & \dots & 0 & \\ \dots & & & & & & & & & \\ \beta_i & \dots & 0 & 0 & -1 & \alpha_i & 0 & \dots & 0 & \\ \dots & & & & & & & & & \\ \beta_{I-1} & \dots & 0 & 0 & 0 & 0 & 0 & -1 & \alpha_{I-1} & \\ 0 & \dots & 0 & 0 & 0 & 0 & 0 & a_I & -c_I & \text{other terms} \end{pmatrix}. \tag{6.15}$$

Step 2. Transformation of the matrix of system (6.12) to an almost diagonal form. Let us write the internal part of system (6.12) in the form:

$$\begin{cases} -c_1\varphi_{k_1} + b_1\varphi_2 = -f_1 + \text{other terms}, \\ p_i\varphi_{k_1} - \varphi_i + q_i\varphi_{k_2} = -s_i, \quad i = 2, \dots, I-1, \\ a_I\varphi_{k_2} - c_I\varphi_{I-1} = -f_I + \text{other terms}, \end{cases} \tag{6.16}$$

where

$$p_i = \alpha_i p_{i+1} + \gamma_i, \quad q_i = \alpha_i q_{i+1},$$

$$s_i = \alpha_i s_{i+1} + \beta_i, \quad i = I-3, \dots, 2 \tag{6.17}$$

and

$$p_{I-2} = \gamma_{I-2}, \quad q_{I-2} = \alpha_{I-2}, \quad s_{I-2} = \beta_{I-2}. \tag{6.18}$$

Now matrix (6.15) is reduced to the following one:

$$\begin{pmatrix} -c_1 & b_1 & 0 & 0 & 0 & 0 & 0 & \dots & 0 & \text{other terms} \\ p_2 & -1 & 0 & 0 & 0 & 0 & 0 & \dots & q_2 & \\ \dots & & & & & & & & & \\ p_i & \dots & 0 & 0 & -1 & 0 & 0 & \dots & q_i & \\ \dots & & & & & & & & & \\ p_{I-1} & \dots & 0 & 0 & 0 & 0 & 0 & -1 & q_{I-1} & \\ 0 & \dots & 0 & 0 & 0 & 0 & 0 & a_I & -c_I & \text{other terms} \end{pmatrix}. \tag{6.19}$$

Step 3. Determination of the new values of φ at the boundary nodes. For any branch we substitute the second equation ($i = 2$) from (6.16) into the first one, and the $(I-1)$-th equation to the last one. We obtain

$$(b_{k_1}p_2 - c_{k_1})\,\varphi_{k_1} + b_{k_1}q_2\varphi_{k_2} = -b_{k_1}s_2 - f_{k_1} + \text{other terms},$$

$$(a_{k_2} - c_{k_2} q_{I-1})\, \varphi_{k_2} - c_{k_2} p_{I-1} \varphi_{k_1} = c_{k_2} s_{I-1} - f_{k_2} + \text{other terms}. \tag{6.20}$$

Let us consider the first and the last equations in (6.20). We see that only the boundary nodes enter these equations. "Other terms" now also contain only the corresponding boundary nodes. Therefore, the boundary nodes form a complete system which allows us to find the unknowns φ in all boundary nodes.

Step 4. Determination of new values in the internal nodes. When the values of φ are found in all boundary nodes, we can obtain new values of φ in the internal nodes for all branches using the corresponding internal equations from system (6.16).

This algorithm is applicable for an arbitrary connection of subsystems.

7. Annexe 2. Cross section area

To have a well posed problem, we need to impose an additional condition of flux conservation at the branching point. Suppose that there are two branches above the branching point. Then

$$dS\frac{\partial C}{\partial x} = d_1 S_1 \frac{\partial C_1}{\partial x} + d_2 S_2 \frac{\partial C_2}{\partial x}, \tag{7.1}$$

where d_1 and d_2 are the diffusion coefficients at each branch, C_1 and C_2 are the concentrations, S is the cross section area below the branching, S_1 and S_2 are the cross section areas above the branching.

We recall that we model a three dimensional plant by a one-dimensional problem. The "memory" about the finite diameter of branches is contained in the effective diffusion coefficient which is proportional to the cross section area. Therefore, to specify the relations between the diffusion coefficients we should begin with the cross sections of the branches.

A trunk width growth occurs because of proliferation of cambium cells as a result of the action of auxin and other compounds descending along the phloem, the narrow layer of plant tissue exterior to the cambium. Consider cuts of the trunk right above and right under the branching, assuming for simplicity that there are two branches above the branching point. Denote by R the radius of the trunk below the branching and by R_1, R_2 the radii above it. Consider a chemical species that determines the proliferation of cambium cells. Let A_1 be its amount in the unit height of the phloem of the first branch, A_2 of the second branch, and A of the trunk below the branching. If we neglect its consumption in the relatively small area between the upper and the lower cut, then

$$A = A_1 + A_2. \tag{7.2}$$

We suppose that the rate of proliferation of cambium cells is proportional to the concentration of this chemical compound. Then the rate of radius growth is proportional to its concentration in the unit length of the perimeter:

$$\frac{dR_1}{dt} = \frac{kA_1}{R_1}, \quad \frac{dR_2}{dt} = \frac{kA_1}{R_2}, \quad \frac{dR}{dt} = \frac{kA}{R}. \tag{7.3}$$

Taking into account (7.2), we obtain

$$\frac{dR^2}{dt} = \frac{dR_1^2}{dt} + \frac{dR_2^2}{dt}. \tag{7.4}$$

Let S_1 be the cross section area of the first branch, S_2 of the second branch, and S of the trunk below the branching. Then from the last equality we obtain

$$\frac{dS}{dt} = \frac{dS_1}{dt} + \frac{dS_2}{dt}. \tag{7.5}$$

Integrating this equation, we obtain

$$S(t) = S_1(t) + S_2(t) + (S(0) - S_1(0) - S_2(0)).$$

For large trees the initial values of the cross section areas are much less than their current values. Therefore, we obtain the approximate equality

$$S(t) \approx S_1(t) + S_2(t). \tag{7.6}$$

This means that the cross section area is the same below and above the branching.

This relation was derived in [**13**] and independently in [**4**]. It is interesting to note that, as the author of [**13**] indicates, Leonardo da Vinci had made this observation about the conservation of cross section areas in trees.

FIGURE 35. Conservation of cross sections.

We have verified this relation by measuring images of trees. Usually it is satisfied within a few percent if the tree is not damaged by natural factors or by artificial shaping. For the examples in Figure 35 we have

a) $r_1 = 6, r_2 = 7, r = 9$, $r_1^2 + r_2^2 = 85, r^2 = 81$,
b) $r_1 = 9, r_2 = 10, r = 13.5$, $r_1^2 + r_2^2 = 181, r^2 = 182.25$,
c) $r_1 = 8.5, r_2 = 11.5, r = 14.5$, $r_1^2 + r_2^2 = 204.5, r^2 = 210.25$,
d) $r_1 = 5, r_2 = 8, r_3 = 9.5, r = 13$, $r_1^2 + r_2^2 + r_3^2 = 179.25, r^2 = 169$.

Conservation of the cross section area remains valid for any number of branches.

Suppose that equality (7.6) is satisfied. Then (7.1) is satisfied if $d = d_1 = d_2$ and

$$\frac{\partial C}{\partial x} = \frac{\partial C_1}{\partial x} = \frac{\partial C_2}{\partial x}.$$

In this case the solution of problem (2.1)-(2.4) will be exactly the same in the case with branching as in the case without branching. In other words, branching does not

change the plant growth. The nutrients in the xylem are distributed proportionally to cross section areas. The production of metabolites by the plant and their concentrations in the phloem is proportional to the fluxes in the xylem. The fluxes in the phloem preserve the equality of cross section areas, which in their turn determine the fluxes in the xylem. This feedback mechanism regulates fluxes in plants.

Equality (7.6) is satisfied for large time. For young plants, it is not usually satisfied. We can consider the limiting case where all branches have the same cross section area. In the case of two branches, we put $S = S_1 = S_2$. We obtain from (7.1)

$$\frac{\partial C}{\partial x} = \frac{\partial C_1}{\partial x} + \frac{\partial C_2}{\partial x}.$$

This equality shows that the concentration gradient decreases after the branching point. We can expect that this will slow down growth.

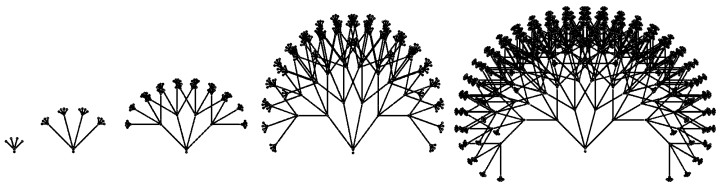

FIGURE 36. Growth with branching.

Figure 36 shows the evolution over time of the growing plant with 4 branches at each branching point. The branching points are not here determined by concentrations of plant hormones but appear in the beginning of each growth period. The final length of the plant in this case is about half that in the case without branching.

8. Annexe 3. 2D stationary solutions

In the 1D case there exist stationary solutions for all lengths L of the interval greater or equal to some minimal value L_0. We discuss here a possible structure of 2D stationary domains. In the stationary case, the model introduced in Section 3 becomes

$$\Delta C = 0, \tag{8.1}$$

$$(x, y) \in \Gamma_i : C = 1, \tag{8.2}$$

$$(x, y) \in \Gamma_e : d\frac{\partial C}{\partial n} = -Cg(R). \tag{8.3}$$

The equation for R at the external boundary yields the equation

$$Cg(R) = \sigma R. \tag{8.4}$$

It should be completed by the additional condition $R \leq R_0$, which implies that $f(R) = 0$ and the boundary does not move. We recall that $g(R)$ is a linear function: for R less than R_0, $g(R) = aR$. This assumption is not necessary, but it will simplify the analysis below. Then we have from (8.4):

$$R = 0 \tag{8.5}$$

or

$$C_{|_{\Gamma_e}} \equiv C_e = \frac{\sigma}{a}. \tag{8.6}$$

If $R = 0$, then the solution of problem (8.1) - (8.4) is $C \equiv 1$. Obviously, it exists for any domain Ω. We will consider the elliptic boundary-value problem (8.1), (8.2), (8.6). It is well posed and has a unique solution for any bounded domain Ω with a sufficiently smooth boundary, and for any values of the parameters.

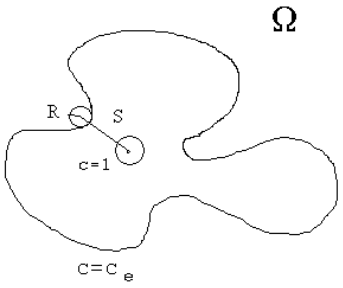

FIGURE 37. Schematic representation of the 2D domain.

Condition (8.3) allows us to find the value of R at the boundary:

$$R = -\frac{d}{\sigma}\,\frac{\partial C}{\partial n}.$$

Therefore we should impose an additional condition on the solution of problem (8.1), (8.2), (8.6):

$$(x, y) \in \Gamma_e : |\frac{\partial C}{\partial n}| \leq \frac{\sigma R_0}{d}\ . \tag{8.7}$$

It can be verified that there exists a solution of problem (8.1), (8.2), (8.6), (8.7) if at each point of the external boundary Γ_e we can construct a circle tangent to the boundary and lying completely outside Ω with the radius R (Figure 37) which satisfies the inequality

$$R \ln(\frac{s-1}{R}) \ \geq \ \frac{d(1-C_e)}{\sigma R_0}.$$

Here s is the distance from the center of this circle to the origin, $s > R + 1$, and the radius of the internal circle is assumed to be 1, but can be changed by scaling. This inequality means that, for a given s, the radius R should not be too small. It can decrease when the distance from the origin increases.

Acknowledgments. The authors are grateful to T. Batygina, C. Godin, N. Morozova, G. Titova, and I. Rudskii for useful discussion. The work was partially supported by the French-Russian program PICS 2092.

References

[1] B. Alberts, D. Bray, J. Lewis, M. Raff, K. Roberts, J. D. Watson. Biologie moléculaire de la cellule. Troisième edition. Médecine-Sciences, Flammarion, Paris, 1995.

[2] B. Alberts, A. Johnson, J. Lewis, M. Raff, K. Roberts, P. Walter. Molecular biology of the cell. 4-th edition, Garland, New York, 2002.

[3] T.B. Batygina. Private communication.

[4] N. Bessonov, V. Volpert. On a problem of plant growth. "Patterns and Waves", A. Abramian, S. Vakulenko, V. Volpert, Eds. St. Petersburg, 2003, pp. 323-337.

[5] F. Boudon, P. Prusinkiewicz, P. Federl, C. Godin, R. Karwowski. Interactive design of bonsai tree models. Eurographics, 22 (2003), No. 3.

[6] R. Escobedo, V. Capasso. Moving bands and moving boundaries with decreasing speed in polymer crystallization. Math. Models Methods Appl. Sci. 15 (2005), No. 3, 325-341.

[7] Yu. Gaponenko, V. Volpert. Numerical simulations of convective Turing structures. "Patterns and Waves", A. Abramian, S. Vakulenko, V. Volpert, Eds. St. Petersburg, 2003, pp. 292-309.

[8] S. Genieys, V. Volpert, P. Auger. On a new mechanism of pattern formation in population dynamics. In press.

[9] C. Godin, Y. Caraglio. A multiscale model of plant topological atructures. J. Theor. Biol. 191 (1998), 1-46.

[10] C. Godin et. al. 4th International workshop on functional-structural plant models. Publication UMR AMAP, 2004.

[11] R. Heller, R. Esnault, C. Lance. Physologie végétale. 2. Développement. 6-ème edition, Dunod, Paris, 1995.

[12] R. V. Jean. Phyllotaxis. A systematic study in plant morphogenesis. Cambridge University Press, New York, 1994.

[13] E.M. Kramer. A mathematical model of auxin-mediated radial growth in trees. J. Theor. Biol., 208 (2001), 387-397.

[14] Y. L. Levy, C. Dean. The transition to flowering. The Plant Cell, 10 (1998), 1973-1989.

[15] P. Mazliak. Physiologie végétale. II. Croissance et développement. Hermann, Paris, 1998.

[16] H. Meinhardt The algorithmic beauty of sea shells. Springer, 2003.

[17] J. Murray. Mathematical biology. Introduction 3rd ed, Springer 2001, 575p.

[18] K.J. Niklas. Computer simulations of branching-patterns and their implications on the evolution of plants. In: Some mathematical questions in biology - Plant biology. Lectures on mathematics in the life sciences, Volume 18, 1986, pp. 1-50. AMS, Providence.

[19] P.H. Raven, R.F. Evert, S.E. Eichhorn. Biologie végétale. 6-ème edition, De Boeck Université, Paris, 2000.

[20] D. Reinhardt, E.-R. Pesce, P. Stieger, T. Mandel, K. Baltensperger, M. Bennett, J. Traas, J.C. Friml. Regulation of phyllotaxis by polar auxin transport. Nature 426, 255 - 260 (2003).

[21] D'Arcy Thompson. On growth and forms. The complete revised edition. Dover, New York, 1992.

[22] A. Turing. The chemical basis of morphogenesis. Phil. Trans. R. Soc. Lond. B 237 (1952), 37-72.

[23] L. Wolpert. Principles of development. Second Edition. Oxford University Press, Oxford, 2002.

Addresses:

N. Bessonov
Institute of Mechanical Engineering Problems, 199178 Saint Petersburg, Russia
e-mail: bessonov1@microm.ipme.ru

V. Volpert
Institute of Mathematics, UMR 5208 CNRS, Université Lyon 1, 69622 Villeurbanne, France
e-mail: volpert@maply.univ-lyon1.fr

Institute of Mechanical Engineering Problems, Saint Petersburg, Russia
E-mail address: bessonov1@microm.ipme.ru

Mathématiques Appliquées, Université Lyon 1, UMR 5585 CNRS, 69622 Villeurbanne, France
E-mail address: volpert@maply.univ-lyon1.fr